# 9

# Smooth point asymptotics

After discussing the overall framework of ACSV in Chapter 7, and the computational tools needed to carry out the analysis in Chapter 8, we are now ready to prove asymptotic theorems. As usual, we begin with a convergent Laurent expansion $F(\boldsymbol{z}) = \sum_{\boldsymbol{r}\in\mathbb{Z}^d} a_{\boldsymbol{r}}\boldsymbol{z}^{\boldsymbol{r}}$ in some domain $\mathcal{D} \subset \mathbb{C}^d$ and try to determine asymptotic behavior of $a_{\boldsymbol{r}}$ as $\boldsymbol{r} \to \infty$ with the normalized vector $\hat{\boldsymbol{r}} = \frac{\boldsymbol{r}}{|\boldsymbol{r}|} = \frac{\boldsymbol{r}}{|r_1|+\cdots+|r_d|}$ restricted to compact sets. In this chapter we give results when dominant asymptotic behavior is determined by the local behavior of $F$ near a finite set of points where its set of singularities $\mathcal{V}$ forms a manifold. Typically we assume $F$ is rational, although we also state results when $F$ is meromorphic.

**Remark 9.1.** The smoothness assumption of this chapter is *generic*, meaning (for instance) that it holds for all rational functions except for those whose coefficients lie in a fixed proper algebraic set depending only on the degree of the denominator. Although this might suggest that every example encountered in practice is handled by the techniques of this chapter, non-generic behavior does occur in many combinatorial applications. Nonetheless, a large fraction of the multivariate generating functions encountered by the authors can be handled by the techniques presented here, without going into the more general theory of Chapters 10 and 11.

### The Main Results of Smooth ACSV

We begin by stating the main theorems of this chapter. Let $F(\boldsymbol{z}) = P(\boldsymbol{z})/Q(\boldsymbol{z})$ be the ratio of coprime polynomials, where $Q \in \mathbb{C}[\boldsymbol{z}]$ has square-free part $\tilde{Q}$ (equal to the product of its distinct irreducible factors). Recall from past chapters that $\boldsymbol{w} \in \mathbb{C}_*^d$ is a *smooth critical point* for the direction $\hat{\boldsymbol{r}} \in \mathbb{R}^d$ if and only if $(\nabla\tilde{Q})(\boldsymbol{w}) \neq \mathbf{0}$ and

$$\tilde{Q}(\boldsymbol{w}) = \hat{r}_i w_d \tilde{Q}_{z_d}(\boldsymbol{w}) - \hat{r}_d w_i \tilde{Q}_{z_i}(\boldsymbol{w}) = 0 \qquad (1 \le i \le d-1). \tag{9.1}$$



https://doi.org/10.1017/9781108874144.014 Published online by Cambridge University Press

The case when the direction vector $\hat{\boldsymbol{r}}$ is the zero vector is trivial, so we always assume that $\hat{\boldsymbol{r}}$ has a non-zero coordinate. When the series expansion of $F$ under consideration is a power series we can further assume the stronger condition that $\hat{\boldsymbol{r}}$ has no zero coordinates, because asking for terms where (say) $r_d = 0$ corresponds to extracting terms from the $(d-1)$-variate series obtained by setting $z_d = 0$. In this case, because our results hold only for critical points with non-zero coordinates, the smooth critical point equations imply that *none* of the partial derivatives of $\tilde{Q}$ vanish.

For Laurent expansions, on the other hand, there are combinatorially interesting cases where $\hat{\boldsymbol{r}}$ has zero coordinates. Even so, if there are to be smooth critical points with non-zero coordinates then the critical point equations imply the existence of a coordinate $k$ such that $r_k \neq 0$ and $\tilde{Q}_{z_k}(\boldsymbol{w}) \neq 0$. Without loss of generality, we may assume this coordinate $k$ is the final coordinate $d$.

Consider a Laurent expansion of $F$ with domain of convergence $\mathcal{D}$. Theorem 6.44 from Chapter 6 implies that if $\boldsymbol{w}$ is a smooth minimal critical point (see Definition 7.7) for the direction $\hat{\boldsymbol{r}}$ then the hyperplane with normal $\hat{\boldsymbol{r}}$ going through the point $\text{Relog}(\boldsymbol{w})$ is a support hyperplane to $B = \text{Relog}(\mathcal{D})$.

**Definition 9.2** (contributing and nondegenerate points)**.** The smooth minimal critical point $\boldsymbol{w}$ described above is called a ***contributing point*** for the direction $\hat{\boldsymbol{r}}$ if $\hat{\boldsymbol{r}}$ points away from $B$ at $\text{Relog}(\boldsymbol{w})$, meaning $\boldsymbol{x} \cdot \hat{\boldsymbol{r}} < \text{Relog}(\boldsymbol{w}) \cdot \hat{\boldsymbol{r}}$ for all $\boldsymbol{x} \in B$. Recall that the point $\boldsymbol{w}$ is nondegenerate if the Hessian matrix $\mathcal{H}$ defined by Lemma 8.22 in Chapter 8 is nonsingular with $H = \tilde{Q}$.

**Remark 9.3.** If we consider the power series expansion of $F(\boldsymbol{z})$, where $\hat{\boldsymbol{r}}$ has positive coordinates, then every smooth minimal critical point is contributing. Recall that nondegeneracy is equivalent to previous definitions in terms of the Hessian of the height function $h(\boldsymbol{z}) = -\boldsymbol{r} \cdot \log \boldsymbol{z}$ restricted to $\mathcal{V}$.

Definition 9.2 is constructed so that contributing points are minimizers of the height function $h_{\hat{\boldsymbol{r}}}$ on $\overline{\mathcal{D}}$, which turn out to be the points determining asymptotic behavior. Conversely, non-contributing smooth minimal critical points are *maximizers* of $h_{\hat{\boldsymbol{r}}}$ on $\overline{\mathcal{D}}$; see Figure 9.1.

**Exercise 9.1.** Which of the components of the complement of the amoeba in Figure 9.1 have a contributing point in the direction $(1, -1)$?

We break our main result into three versions, depending on the assumptions required and the proof techniques used. Our first version is the most restrictive, however it still holds in a wide variety of applications and has the advantage that it can be derived purely through complex analysis and classical saddle point techniques, without the need for the homological framework of

https://doi.org/10.1017/9781108874144.014 Published online by Cambridge University Press

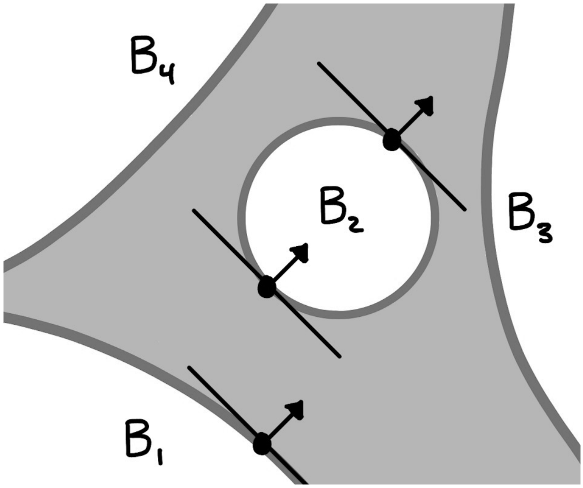


Figure 9.1 The amoeba complement component $B_1$, corresponding to a power series expansion, has one point on its boundary where its support hyperplane has normal $\boldsymbol{r} = (1, 1)$, which corresponds to contributing points. On the other hand, the component $B_2$ has two boundary points with support hyperplanes having normals $\boldsymbol{r} = (1, 1)$, only one of which (the upper-most one) corresponds to contributing singularities.

Chapter 7. In order to simplify our presentation, we begin by stating it in the common special case where $Q$ is square-free and there is a single minimal contributing point.

**Theorem 9.4** (Main Theorem of Smooth ACSV (Local Version, Square-Free Case))**.** *Let $F(\boldsymbol{z}) = P(\boldsymbol{z})/Q(\boldsymbol{z})$ be the ratio of coprime polynomials $P$ and $Q$ with convergent Laurent expansion $F(\boldsymbol{z}) = \sum_{\boldsymbol{r}\in\mathbb{Z}^d} a_{\boldsymbol{r}} \boldsymbol{z}^{\boldsymbol{r}}$. Suppose that there is a compact set $\mathcal{R} \subset \mathbb{R}^d$ of non-zero directions such that if $\hat{\boldsymbol{r}}$ lies in $\mathcal{R}$ then $F$ has a smooth strictly minimal nondegenerate contributing point $\boldsymbol{w} = \boldsymbol{w}(\hat{\boldsymbol{r}}) \in \mathbb{C}_*^d$, and let $\mathcal{H} = \mathcal{H}(\hat{\boldsymbol{r}})$ be the Hessian matrix defined by* (8.7) *and* (8.8) *when $H = Q$. If $Q_{z_d}(\boldsymbol{w}) \neq 0$ then*

$$a_{\boldsymbol{r}} \approx \Phi_{\boldsymbol{w}}(\boldsymbol{r})$$

*uniformly as $\boldsymbol{r} \to \infty$ with $\hat{\boldsymbol{r}} \in \mathcal{R}$, where $\Phi_{\boldsymbol{w}}(\boldsymbol{r})$ is an asymptotic series*

$$\Phi_{\boldsymbol{w}}(\boldsymbol{r}) = \boldsymbol{w}^{-\boldsymbol{r}} |r_d|^{(1-d)/2} \frac{(2\pi)^{(1-d)/2} \operatorname{sgn}(r_d)}{\sqrt{\det(\operatorname{sgn}(r_d)\mathcal{H})}} \sum_{\ell=0}^{\infty} C_\ell(\hat{\boldsymbol{r}}) r_d^{-\ell}. \tag{9.2}$$

*The square-root of the matrix determinant is the product of the principal branch square-roots of its eigenvalues (which will have nonnegative real parts). The*

https://doi.org/10.1017/9781108874144.014 Published online by Cambridge University Press

*constants $C_\ell$ are explicitly computable in terms of the derivatives of $P(\boldsymbol{z})$ and $Q(\boldsymbol{z})$ evaluated at $\boldsymbol{z} = \boldsymbol{w}(\hat{\boldsymbol{r}})$. In particular,*

$$C_0 = \frac{P(\boldsymbol{w})}{-w_d Q_d(\boldsymbol{w})}. \tag{9.3}$$

□

Theorem 9.4 is a special case of the following, which holds for poles of general order.

**Theorem 9.5** (Main Theorem of Smooth ACSV (Local Version))**.** *Let $F(\boldsymbol{z}) = P(\boldsymbol{z})/Q(\boldsymbol{z})$ be the ratio of coprime polynomials with convergent Laurent expansion $F(\boldsymbol{z}) = \sum_{\boldsymbol{r}\in\mathbb{Z}^d} a_{\boldsymbol{r}} \boldsymbol{z}^{\boldsymbol{r}}$. Suppose there exists a compact set $\mathcal{R} \subset \mathbb{R}^d$ of non-zero directions such that if $\hat{\boldsymbol{r}}$ lies in $\mathcal{R}$ then $F$ has a smooth strictly minimal nondegenerate contributing point $\boldsymbol{w} = \boldsymbol{w}(\hat{\boldsymbol{r}}) \in \mathbb{C}_*^d$, and let $\mathcal{H} = \mathcal{H}(\hat{\boldsymbol{r}})$ be the Hessian matrix defined by* (8.7) *and* (8.8) *when $H = \tilde{Q}$. If $(\partial_d^p Q)(\boldsymbol{w}) \neq 0$ and $(\partial_d^q Q)(\boldsymbol{w}) = 0$ for all $0 \leq q < p$ then*

$$a_{\boldsymbol{r}} \approx \Phi_{\boldsymbol{w}}(\boldsymbol{r})$$

*uniformly as $\boldsymbol{r} \to \infty$ with $\hat{\boldsymbol{r}} \in \mathcal{R}$, where $\Phi_{\boldsymbol{w}}(\boldsymbol{r})$ is an asymptotic series*

$$\Phi_{\boldsymbol{w}}(\boldsymbol{r}) = \boldsymbol{w}^{-\boldsymbol{r}} |r_d|^{p-1+(1-d)/2} \frac{(2\pi)^{(1-d)/2}\operatorname{sgn}(r_d)^p}{\sqrt{\det(\operatorname{sgn}(r_d)\,\mathcal{H})}} \sum_{\ell=0}^{\infty} C_\ell(\hat{\boldsymbol{r}}) r_d^{-\ell}. \tag{9.4}$$

*The square-root of the matrix determinant is the product of the principal branch square-roots of its eigenvalues (which will have nonnegative real parts). The constants $C_\ell$ are explicitly computable in terms of the derivatives of $P(\boldsymbol{z})$ and $Q(\boldsymbol{z})$ evaluated at $\boldsymbol{z} = \boldsymbol{w}(\hat{\boldsymbol{r}})$. In particular,*

$$C_0 = \frac{(-1)^p P(\boldsymbol{w}) p}{w_d^p (\partial_d^p Q)(\boldsymbol{w})}.$$

*If $\boldsymbol{w}$ is a finitely minimal point (instead of being strictly minimal) such that all points in the set $\mathbf{W}(\hat{\boldsymbol{r}}) = T(\boldsymbol{w}) \cap \mathcal{V}$ vary smoothly with $\hat{\boldsymbol{r}}$ in $\mathcal{R}$ and are contributing points satisfying the conditions above then*

$$a_{\boldsymbol{r}} \approx \sum_{\boldsymbol{y}\in\mathbf{W}(\hat{\boldsymbol{r}})} \Phi_{\boldsymbol{y}}(\boldsymbol{r}),$$

*where each $\Phi_{\boldsymbol{y}}$ is given by* (9.4).

**Exercise 9.2.** What, in general, can go wrong pulling a factor of $\operatorname{sgn}(r_d)^{d-1}$ out of the square-root in the denominator of (9.4)?

**Remark 9.6.** An explicit (but unwieldy) formula for all coefficients in (9.4) is given in Section 9.4 below. If $Q = H^p$ for some square-free $H$ with $\nabla H$ nonvanishing at $\boldsymbol{w}$ then

$$C_0 = \frac{(-1)^p P(\boldsymbol{w})}{(p-1)!\,(w_d \partial_d H(\boldsymbol{w}))^p}.$$

**Remark 9.7.** Our surgery approach below singles out the coordinate $z_d$ for a residue computation, leading to an asymptotic expansion in powers of the non-zero coordinate $r_d$. With some extra work, the Fourier–Laplace integral used to deduce asymptotics can be modified to provide an asymptotic series in powers of $|\boldsymbol{r}|$, giving an expansion of the form

$$\Phi_{\boldsymbol{w}}(\boldsymbol{r}) = \boldsymbol{w}^{-\boldsymbol{r}} \frac{1}{\sqrt{\det(2\pi|\boldsymbol{r}|\,\mathcal{H}')}} \sum_{\ell=0}^{\infty} C'_\ell(\hat{\boldsymbol{r}})|\boldsymbol{r}|^{-\ell} \tag{9.5}$$

for a new Hessian matrix $\mathcal{H}'$. We leave details of such symmetric formulae to Chapter 10, where asymptotics are computed using multivariate residue forms that do not privilege individual coordinates.

**Remark 9.8.** If $\mathcal{R} = \{\boldsymbol{s}\}$ contains a single point with $s_d > 0$ then $\boldsymbol{r} = n\boldsymbol{s}$ and

$$\Phi_{\boldsymbol{w}}(n\boldsymbol{s}) \approx \boldsymbol{w}^{-n\boldsymbol{s}}\; n^{p-1+(1-d)/2} \frac{(2\pi)^{(1-d)/2}}{\sqrt{\det(\mathcal{H})}} \sum_{\ell=0}^{\infty} D_\ell n^{-\ell}$$

for constants $D_\ell$ with $D_0 = (s_d)^{p-d} C_0$.

**Example 9.9.** The hypotheses of Theorem 9.5 can be simplified for bivariate power series. In particular, suppose that $F(x,y) = \frac{P(x,y)}{Q(x,y)} = \sum_{i,j\geq 0} a_{ij} x^i y^j$ admits a strictly minimal critical point $\boldsymbol{w} = \boldsymbol{w}(\boldsymbol{r}) \in \mathbb{C}_*^2$ that varies smoothly as $\hat{\boldsymbol{r}}$ varies in a compact neighborhood $\mathcal{R}$ of directions. If both $P(x,y)$ and the expression

$$\underline{Q}(x,y) = -xy^2 Q_y^2 Q_x - x^2 y Q_y Q_x - x^2 y^2 (Q_y^2 Q_{xx} + Q_x^2 Q_{yy} - 2Q_x Q_y Q_{xy}) \tag{9.6}$$

are non-zero when $(x,y) = \boldsymbol{w}(\hat{\boldsymbol{r}})$ for each $\hat{\boldsymbol{r}} \in \mathcal{R}$ then

$$\begin{aligned} a_{r,s} &\sim \frac{P(x,y)}{-yQ_y} \frac{1}{\sqrt{2\pi}}\, x^{-r} y^{-s} \sqrt{\frac{(-yQ_y)^3}{s\underline{Q}}} \\ &= \frac{P(x,y)}{-xQ_x} \frac{1}{\sqrt{2\pi}}\, x^{-r} y^{-s} \sqrt{\frac{(-xQ_x)^3}{r\underline{Q}}} \end{aligned} \tag{9.7}$$

as $|\boldsymbol{r}| \to \infty$ after setting $(x,y) = \boldsymbol{w}(\hat{\boldsymbol{r}})$, uniformly over $\hat{\boldsymbol{r}} \in \mathcal{R}$. ◁

**Exercise 9.3.** Prove (9.7) by simplifying (9.2) in the bivariate case.

**Example 9.10** (binomial coefficients continued)**.** If $F(x, y) = 1/(1-x-y)$ then the coefficient of $x^r y^s$ in the power series expansion of $F$ is $\binom{r+s}{s}$. Solving the smooth critical point equations yields the unique critical point

$$\boldsymbol{w} = \left(\frac{r}{r+s}, \frac{s}{r+s}\right) = (\hat{r}, \hat{s}),$$

which is strictly minimal by Lemma 6.41. We obtain

$$\binom{r+s}{s} \sim \frac{(r+s)^{r+s}}{r^r s^s} \sqrt{\frac{r+s}{2\pi r s}}$$

as $r, s \to \infty$ with $r/s$ bounded away from zero and infinity. For example, the central binomial coefficients given by $r = s = n$ satisfy $\binom{2n}{n} \sim 4^n / \sqrt{\pi n}$. ◁

**Example 9.11** (Delannoy numbers continued)**.** If $F(x, y) = 1/(1-x-y-xy)$ then we have the critical points

$$(x_*, y_*) = \left(\frac{\sqrt{r^2+s^2}-s}{r}, \frac{\sqrt{r^2+s^2}-r}{s}\right) \text{ or } \left(\frac{-\sqrt{r^2+s^2}-s}{r}, \frac{-\sqrt{r^2+s^2}-r}{s}\right),$$

the first of which is strictly minimal by Lemma 6.41. Writing $d = \sqrt{r^2+s^2}$, we directly compute

$$a_{rs} \sim \left(\frac{r}{d-s}\right)^r \left(\frac{s}{d-r}\right)^s \sqrt{\frac{rs\,(d^2+(r-s))}{2\pi\,(r+s-d)\,(d^2+d(r-s))}}$$

as $r, s \to \infty$ with $r/s$ bounded away from zero and infinity. ◁

We give a proof of Theorem 9.5 in Section 9.1 using the *surgery method* for ACSV, which works in the presence of smooth finitely minimal contributing points. Although the requirement of finite minimality makes proofs simpler, it is computationally difficult to check, and rules out cases that can be handled by our other results. In Section 9.2 we use more advanced techniques (including the theory of *hyperbolic polynomials* developed in Chapter 11) to prove an extension of Theorem 9.5 that ignores non-critical points and only requires that the torus $T(\boldsymbol{w})$ contains a *finite number of critical points*. This gives a large computational advantage, because generically there are a finite number of critical points described by a zero-dimensional algebraic set.

**Theorem 9.12** (Main Theorem of Smooth ACSV (Minimal Point Version))**.** *Let $F(\boldsymbol{z}) = P(\boldsymbol{z})/Q(\boldsymbol{z})$ be the ratio of coprime polynomials with convergent Laurent expansion $F(\boldsymbol{z}) = \sum_{\boldsymbol{r} \in \mathbb{Z}^d} a_{\boldsymbol{r}} \boldsymbol{z}^{\boldsymbol{r}}$. Suppose there exists a compact set $\mathcal{R} \subset \mathbb{R}^d$ of non-zero directions such that $F$ has a smooth minimal nondegenerate contributing point $\boldsymbol{w} = \boldsymbol{w}(\hat{\boldsymbol{r}}) \in \mathbb{C}_*^d$ whenever $\hat{\boldsymbol{r}} \in \mathcal{R}$. If the set $\mathbf{W}(\hat{\boldsymbol{r}})$ of solutions* *to* (9.1) *with the same coordinatewise modulus as* $\mathbf{w}(\hat{\mathbf{r}})$ *is finite and contains only smooth nondegenerate contributing points that vary smoothly with* $\hat{\mathbf{r}}$ *then*

$$a_{\mathbf{r}} \approx \sum_{\mathbf{y} \in \mathbf{W}(\hat{\mathbf{r}})} \Phi_{\mathbf{y}}(\mathbf{r}), \tag{9.8}$$

*uniformly as* $\mathbf{r} \to \infty$ *with* $\hat{\mathbf{r}} \in \mathcal{R}$, *where* $\Phi_{\mathbf{y}}$ *is defined in* (9.4).

**Example 9.13** (negative binomial coefficients). If $F(x, y) = -x/(1-x-y)$ then the coefficient of $x^{-r}y^s$ in the Laurent series expansion of $F$ converging in the domain $1 + |y| < |x|$ is $(-1)^s\binom{r}{s}$. There is a unique critical point

$$\mathbf{w} = \left(\frac{-r}{-r+s}, \frac{s}{-r+s}\right),$$

where now, because $r > s$, the first coordinate of $\mathbf{w}$ is positive while the second is negative. This point is minimal, since it lives on the boundary $\{(x, y) \in \mathbb{C}^2 : 1 + |y| = |x|\}$ of the domain of convergence of this Laurent series, and contributing. Ultimately, we obtain

$$[x^{-r}y^s]F \sim (-1)^s \frac{r^r}{(r-s)^{r-s}s^s}\sqrt{\frac{r}{2\pi(r-s)s}}.$$

Note that if we replace $x$ by $1/x$ in $F$, we obtain $G = 1/(1 - x + xy)$, whose $(r, s)$-coefficient is $(-1)^s\binom{r}{s}$. This is consistent with the usual identity

$$\binom{-r}{s} = (-1)^s\binom{r+s-1}{s}$$

for binomial coefficients when $r, s > 0$. Replacing $y$ by $-y$, we are led back to the generating function $1/(1 - x - xy)$ for binomial coefficients examined above. ◁

**Example 9.14** (Chebyshev polynomials). Let $F(z, w) = 1/(1-2zw+w^2)$ be the generating function for ***Chebyshev polynomials*** of the second kind [Com74]. To use Theorem 9.12 for an arbitrary direction $(r, s)$ with nonnegative indices and $r/s \in (0, 1)$, we first compute the critical points $\mathbf{w}_\pm = \left(i\left(\beta - \beta^{-1}\right)/2, i\beta\right)$, where $\beta = \pm\sqrt{\frac{s-r}{s+r}}$. These points are minimal by Corollary 6.36 because if we substitute $(z, w) = (tx, ty)$ in the denominator then $|2xy - y^2|$ is at most $t^2\left(1 - \beta^2 + \beta^2\right) < 1$, and hence $T(t\mathbf{w}_\pm) \cap \mathcal{V} = \varnothing$ for all $t \in (0, 1)$. These points are contributing because any smooth minimal critical points are contributing for power series expansions.

Summing the asymptotic contributions given by the two points implies

$$a_{rs} \sim \sqrt{\frac{2}{\pi}}(-1)^{(s-r)/2}\left(\frac{2r}{\sqrt{s^2-r^2}}\right)^{-r}\left(\sqrt{\frac{s-r}{s+r}}\right)^{-s}\sqrt{\frac{s+r}{r(s-r)}}$$

https://doi.org/10.1017/9781108874144.014 Published online by Cambridge University Press

when $r + s$ is even, while $a_{rs} = 0$ when $r + s$ is odd. These asymptotics are uniform as $r/s$ varies over any compact subset of $(0, 1)$. ◁

**Exercise 9.4.** Redo Examples 9.13 and 9.14 using Theorem 9.5 instead of Theorem 9.12. What extra conditions do you need to check?

In the presence of minimal critical points we do not need to rule out the critical points at infinity (CPAI) discussed in previous chapters. However, if we do rule out CPAI then Theorem 7.20 applies and we get the following.

**Theorem 9.15** (Main Theorem of Smooth ACSV (No CPAI Version))**.** *Suppose that, as $\hat{\boldsymbol{r}}$ varies over a compact set $\mathcal{R} \subset \mathbb{R}^d$ of non-zero directions, the function $F$ has no CPAI with height at least $M \in \mathbb{R}$, and that the set $\mathbf{W} = \mathbf{W}(\hat{\boldsymbol{r}})$ of critical points with height larger than $M$ is finite and consists of smooth non-degenerate points. Then there exist $\kappa_{\boldsymbol{w}} \in \mathbb{Z}$ for $\boldsymbol{w} \in \mathbf{W}$ with*

$$a_{\boldsymbol{r}} \approx \sum_{\boldsymbol{w} \in \mathbf{W}} \kappa_{\boldsymbol{w}} \, \Phi_{\boldsymbol{w}}(\boldsymbol{r}) + O(e^{M|\boldsymbol{r}|}) \,, \tag{9.9}$$

*where each $\Phi_{\boldsymbol{w}}$ is the asymptotic series defined by* (9.4).

To determine dominant asymptotic behavior, it is necessary to identify the highest critical points $\boldsymbol{w}$ with non-zero coefficients $\kappa_{\boldsymbol{w}}$. This seems to be a very difficult task in general, but we can say more in some circumstances. For instance, $\kappa_{\boldsymbol{w}} = 1$ for any smooth minimal contributing points, and if $a_{\boldsymbol{r}}$ is not eventually zero and $M = -\infty$ then at least one $\kappa_{\boldsymbol{w}}$ is non-zero. If the exponential growth of a sequence can be determined or bounded using other means, this can also be used to identify the highest coefficients which are non-zero, and thus pin down asymptotics up to these unknown integers.

Although Theorem 9.15 is the most abstract of our main theorems, it follows directly from the large amount of technical background in Chapter 7 and the appendices, and some computations from the proof of Theorem 9.12 below.

*Proof of Theorem 9.15* Fix a direction $\hat{\boldsymbol{r}}$. In the absence of CPAI at height $M$ or above, Theorem 7.20 in Chapter 7 shows that, for some $\varepsilon > 0$, the homology group $H_d(\mathcal{M}, \mathcal{M}_{\leq M-\varepsilon})$ has a basis indexed by the critical points $\boldsymbol{\sigma}_1, \ldots, \boldsymbol{\sigma}_m$ for $Q$ whose elements are smooth cycles $\gamma_j$ such that $h_{\hat{\boldsymbol{r}}}$ attains its maximum on $\gamma_j$ at $\boldsymbol{\sigma}_j$ and

$$a_{\boldsymbol{r}} = \sum_{j=1}^{m} \frac{\kappa_j}{(2\pi i)^{d-1}} \int_{\gamma_j} \operatorname{Res}\Big(F(\boldsymbol{z})\boldsymbol{z}^{-\boldsymbol{r}-\mathbf{1}} \, d\boldsymbol{z}\Big) + O(e^{M|\boldsymbol{r}|}).$$

We will determine this residue integral and its uniform error term with $\hat{\boldsymbol{r}}$ in our proof of Theorem 9.12 below, giving the stated expansion. □

Sections 9.3.1 and 9.3.2 complement the decomposition (9.9) by presenting an algorithm to determine the integer coefficients $k_{\boldsymbol{w}}$ for bivariate series, the only case beyond minimal points and rational functions with linear denominators where we know a general strategy for their calculation. Section 9.3.3 also gives an asymptotic formula for degenerate critical points in the bivariate case. Finally, Section 9.4 ends this chapter with some related results, including explicit formulae for higher-order terms and a coordinate-free formula (9.23) in terms of geometric invariants such as the Gaussian curvature.

## 9.1 Finitely minimal points and the surgery method

To prove Theorem 9.5 we show that the Cauchy integral representation for series coefficients is negligible outside a small neighborhood of $\boldsymbol{w}$, reduce to a lower-dimensional integral using a univariate residue computation, parametrize the simplified integral to obtain a saddle point integral, and apply the theorems of Chapter 5 to the result.

### Localization and residue

We start by assuming that $\mathbf{W}(\hat{\boldsymbol{r}})$ contains a strictly minimal contributing singularity $\boldsymbol{w} = \boldsymbol{w}(\hat{\boldsymbol{r}})$.

**Definition 9.16.** For simplicity, we write $\boldsymbol{v}^\circ = (v_1, \ldots, v_{d-1})$ for any vector $\boldsymbol{v} \in \mathbb{C}^d$.

Our hypotheses imply that $\tilde{Q}_{z_d}(\boldsymbol{w}) \neq 0$, so the implicit function theorem states that $z_d$ is locally analytically parametrized by $\boldsymbol{z}^\circ$ near $\boldsymbol{w}$ on $\mathcal{V}$. More specifically, if $r_d > 0$ and we define $\rho = |w_d|$ then there exist a sufficiently small real number $\delta > 0$, a neighborhood $\mathcal{N}$ of $\boldsymbol{w}^\circ$ in $T(\boldsymbol{w}^\circ)$, and an analytic function $g : \mathcal{N} \to \mathbb{C}$ such that for $\boldsymbol{z}^\circ \in \mathcal{N}$,

(i) $Q(\boldsymbol{z}^\circ, g(\boldsymbol{z}^\circ)) = 0$,
(ii) $\rho \leq |g(\boldsymbol{z}^\circ)| < \rho + \delta$ with equality only if $\boldsymbol{z}^\circ = \boldsymbol{w}^\circ$, and
(iii) $Q(\boldsymbol{z}^\circ, t) \neq 0$ if $t \neq g(\boldsymbol{z}^\circ)$ and $|t - w_d| < \delta$.

If $r_d < 0$ then the same conditions hold except $\boldsymbol{w}$ being contributing means the inequality in (ii) is replaced by $\rho - \delta < |g(\boldsymbol{z}^\circ)| \leq \rho$.

Let $C_1$ denote the circle of radius $\rho - \delta$ centered at the origin of the complex plane and let $C_2$ denote the circle of radius $\rho + \delta$. The fact that $\boldsymbol{w}$ is contributing, combined with the Cauchy integral formula, implies that the series coefficients of interest can be represented by an iterated integral

$$a_{\boldsymbol{r}} = \begin{cases} \left(\frac{1}{2\pi i}\right)^d \int_{\mathbf{T}(\boldsymbol{w}^\circ)} \left[\int_{C_1} F(\boldsymbol{z}^\circ, t) t^{-r_d - 1}\, dt\right] (\boldsymbol{z}^\circ)^{-\boldsymbol{r}^\circ} \frac{d\boldsymbol{z}^\circ}{z_1 \cdots z_{d-1}} & \text{if } r_d > 0 \\ \left(\frac{1}{2\pi i}\right)^d \int_{\mathbf{T}(\boldsymbol{w}^\circ)} \left[\int_{C_2} F(\boldsymbol{z}^\circ, t) t^{-r_d - 1}\, dt\right] (\boldsymbol{z}^\circ)^{-\boldsymbol{r}^\circ} \frac{d\boldsymbol{z}^\circ}{z_1 \cdots z_{d-1}} & \text{if } r_d < 0 \end{cases}. \tag{9.10}$$

In either case, the key observation is that the inner integral is exponentially smaller than $\rho^{-r_d}$ away from $\boldsymbol{w}^\circ$. Indeed, if $r_d > 0$ under our assumptions then for each fixed $\boldsymbol{z}^\circ \neq \boldsymbol{w}^\circ$ the function $f(t) = F(\boldsymbol{z}^\circ, t)$ has radius of convergence greater than $\rho$ and the inner integral is $O((\rho+\varepsilon)^{-r_d})$ for some $\varepsilon > 0$; by continuity of the radius of convergence, a single $\varepsilon > 0$ may be chosen for all compact subsets of $\mathbf{T}(\boldsymbol{w}^\circ)$ not containing $\boldsymbol{w}^\circ$. Similarly, if $r_d < 0$ then the inner integral is $O((\rho + \varepsilon)^{-r_d})$ for some $\varepsilon \in (-\rho, 0)$. Thus,

$$|\boldsymbol{w}^{\boldsymbol{r}} (a_{\boldsymbol{r}} - I)| \to 0 \tag{9.11}$$

exponentially quickly, where $I$ is any integral in (9.10) with $\mathbf{T}(\boldsymbol{w}^\circ)$ replaced by any neighborhood of $\boldsymbol{w}^\circ$ in $\mathbf{T}(\boldsymbol{w}^\circ)$. We now take the neighborhood defining $I$ to be the set $\mathcal{N}$ on which the properties (i)–(iii) for the parametrization $g$ hold, and compare the inner integral in (9.10) to one pushed 'beyond' the singular set. Note that in general we cannot do this without first 'cutting out' the small neighborhood $\mathcal{N}$.

Assume that $r_d > 0$ and compare

$$I = \left(\frac{1}{2\pi i}\right)^d \int_{\mathcal{N}} \left[\int_{C_1} F(\boldsymbol{z}^\circ, t) t^{-r_d - 1}\, dt\right] (\boldsymbol{z}^\circ)^{-\boldsymbol{r}^\circ} \frac{d\boldsymbol{z}^\circ}{z_1 \cdots z_{d-1}}$$

to the integral

$$I' = \left(\frac{1}{2\pi i}\right)^d \int_{\mathcal{N}} \left[\int_{C_2} F(\boldsymbol{z}^\circ, t) t^{-r_d - 1}\, dt\right] (\boldsymbol{z}^\circ)^{-\boldsymbol{r}^\circ} \frac{d\boldsymbol{z}^\circ}{z_1 \cdots z_{d-1}}$$

with the inner contour $C_1$ replaced by $C_2$. Because the points on $C_2$ have larger modulus than $\rho$,

$$\left|\boldsymbol{w}^{\boldsymbol{r}} I'\right| \to 0 \tag{9.12}$$

exponentially quickly. Furthermore, our assumption of strict minimality implies that the common inner integrand of $I$ and $I'$ has a unique pole in the annulus $\rho - \delta \le |t| \le \rho + \delta$, occurring at $t = g(\boldsymbol{z}^\circ)$. If

$$\Psi(\boldsymbol{z}^\circ) = \operatorname{Res}\left(F(\boldsymbol{z}^\circ, t) t^{-r_d - 1}\, ;\, t = g(\boldsymbol{z}^\circ)\right) \tag{9.13}$$

https://doi.org/10.1017/9781108874144.014 Published online by Cambridge University Press

then the difference of $I$ and $I'$ can be computed in terms of $\Psi$. If $r_d < 0$ the argument is the same, with the roles of $C_1$ and $C_2$ reversed, changing the sign in front of the residue integral. Ultimately, we obtain the following, which may be thought of as the computational analog of the fact that one can integrate in relative homology at the expense of an exponentially small error (see Proposition B.10 in Appendix B).

**Theorem 9.17** (reduction to residue integral)**.** *Let*

$$\chi = I - I' = \frac{-\operatorname{sgn}(r_d)}{(2\pi i)^{d-1}} \int_{\mathcal{N}} \Psi(z^\circ)(z^\circ)^{-r^\circ} \frac{dz^\circ}{z_1 \cdots z_{d-1}}, \tag{9.14}$$

*with* $\Psi$ *given by* (9.13). *Assuming the hypotheses of Theorem 9.5 when* $\mathbf{W}(r) = \{w(\hat{r})\}$,

$$|w^r (a_r - \chi)| \to 0$$

*exponentially in* $|r|$, *uniformly as* $r \to \infty$ *with* $\hat{r}$ *varying over* $\mathcal{M}$.

The fact that we can obtain explicit asymptotic expansions is a consequence of the following result.

**Lemma 9.18.** *Under the hypotheses of Theorem 9.5, the residue* $\Psi$ *has the form* $\Psi(z^\circ) = -g(z^\circ)^{-r_d}\Psi_p(z^\circ)$ *where*

$$\Psi_p(z^\circ) = \sum_{k=0}^{p-1} \frac{(r_d + 1)_{(p-k-1)}}{k!(p-k-1)!} R_k(z^\circ). \tag{9.15}$$

*Here* $(a)_{(b)} = a(a-1)\cdots(a-b+1)$ *and*

$$R_k(z^\circ) = (-g(z^\circ))^{-p+k} \lim_{z_d \to g(z^\circ)} \partial_d^k \left((z_d - g(z^\circ))^p F(z)\right).$$

*In particular,* $\Psi_p$ *is a polynomial of degree* $p-1$ *in* $r_d$ *with leading coefficient*

$$(-1)^p g(z^\circ)^{-p}\, p\, \frac{P(z^\circ, g(z^\circ))}{(\partial_d^p Q)(z^\circ, g(z^\circ))}.$$

*Proof* Our assumptions imply that $F(z^\circ, t)$ has a pole of order $p$ at $t = g(z^\circ)$, and (9.15) comes from the classic residue formula

$$\operatorname{Res}\left(F(z^\circ, t)t^{-r_d-1}\,;\, t = g(z^\circ)\right) = \frac{1}{(p-1)!} \lim_{z_d \to g(z^\circ)} \partial_d^{p-1}\left((z_d - g(z^\circ))^p F(z) z_d^{-r_d-1}\right)$$

together with Leibniz's rule for derivatives. The leading term in $r_d$ comes from the summand where $k = 0$. □

**Remark 9.19.** The results of this section only require that $F$ be meromorphic in a neighborhood of the domain of convergence $\mathcal{D}$. If $F$ is locally the ratio of analytic functions $P$ and $Q$ in a neighborhood of $w$ then all formulae are still valid, provided $\tilde{Q}$ is interpreted to be a square-free factorization in the local ring of germs of analytic functions (see Definition 10.42 below).

**Exercise 9.5.** Let $F(x, y) = 1/(e^x + e^y - 1)$. What can you deduce from Theorem 9.5 about the power series coefficients of $F$?

## Proof of Theorem 9.5

Making the change of variables $z_j = w_j e^{i\theta_j}$ for $1 \le j \le d-1$ turns $\chi$ into a saddle point integral

$$\chi = \frac{\operatorname{sgn}(r_d)}{(2\pi)^{d-1}} \boldsymbol{w}^{-\boldsymbol{r}} \int_{\mathcal{N}'} A(\boldsymbol{\theta}) e^{-|r_d|\phi(\theta)} d\boldsymbol{\theta} \tag{9.16}$$

with amplitude $A(\boldsymbol{\theta}) = \Psi_p\left(\boldsymbol{w}^\circ e^{i\boldsymbol{\theta}}\right)$ for $\Psi_p$ defined in (9.15) and phase

$$\begin{aligned}\phi(\boldsymbol{\theta}) &= \frac{r_d}{|r_d|} \log\left(\frac{g\left(\boldsymbol{w}^\circ e^{i\boldsymbol{\theta}}\right)}{w_d}\right) + i\frac{(\boldsymbol{r}^\circ \cdot \boldsymbol{\theta})}{|r_d|} \\ &= \operatorname{sgn}(r_d)\left[\log\left(\frac{g\left(\boldsymbol{w}^\circ e^{i\boldsymbol{\theta}}\right)}{w_d}\right) + i\frac{(\boldsymbol{r}^\circ \cdot \boldsymbol{\theta})}{r_d}\right]\end{aligned}$$

in the variables $\boldsymbol{\theta} = (\theta_1, \dots, \theta_{d-1})$, where $\left(\boldsymbol{w}^\circ e^{i\boldsymbol{\theta}}\right) = \left(w_1 e^{i\theta_1}, \dots, w_{d-1} e^{i\theta_{d-1}}\right)$ and $\mathcal{N}'$ is a neighborhood of the origin in $\mathbb{R}^d$. Lemma 8.21 implies that this integral satisfies the conditions necessary to apply Theorem 5.2 in Chapter 5 (note that the real part of $\phi$ has a strict minimum at the origin by our conditions on $g$). Lemma 8.22 applied to $\operatorname{sgn}(r_d)\phi$ simplifies the Hessian and finishes the proof.

## Modification for finitely minimal points

When $\boldsymbol{w}(\hat{\boldsymbol{r}})$ is finitely minimal then the Cauchy integral decays exponentially away from any element of $\mathbf{W}(\hat{\boldsymbol{r}})$. We can thus restrict the domain of integration to a disjoint union of neighborhoods $\mathcal{N}_k$ around the elements of $\mathbf{W}(\hat{\boldsymbol{r}})$. The residue computation in Theorem 9.17 results in a sum as $k$ varies of integrals over neighborhoods $\mathcal{N}_{\boldsymbol{w}_k}$. The asymptotic contributions of each of the integrals in the sum can be computed in the same way as the strictly minimal case.

## Modification under strong torality hypothesis

Because our residue computations are so explicit, they also hold under the following *strong torality hypothesis*. This hypothesis is important when studying generating functions whose singularities have many symmetries, for instance in the case of quantum random walks (see Exercise 9.12).

**Definition 9.20** (strong torality). We say $Q$ satisfies the ***strong torality hypothesis*** on the torus $\mathbf{T}(\boldsymbol{w})$ if $Q(\boldsymbol{z}) = 0$ and $|z_j| = |w_j|$ for $1 \le j \le d-1$ implies that $|z_d| = |w_d|$.

**Exercise 9.6.** Suppose that the function $Q(x,y) = a + bx + cy + dxy$ is bilinear. What conditions on the constants $a, b, c, d$ are equivalent to strong torality of $Q$?

In the following proposition $g$ is the multivalued function solving for $z_d$ as a function of $\boldsymbol{z}^\circ$; the number of values, counted with multiplicities, is the degree $m$ of $z_d$ in $Q$, except on a lower dimensional set where two values coincide. The multivalued integrand should be interpreted as a sum over all $m$ values.

**Corollary 9.21** (reduction under strong torality). *Suppose $\boldsymbol{w}$ satisfies all of the hypotheses of Theorem 9.5 except that instead of $\boldsymbol{w}$ being finitely minimal, it is minimal and $Q$ satisfies the strong torality hypothesis on $\mathbf{T}(\boldsymbol{w})$. If all poles of $F$ on $\mathbf{T}(\boldsymbol{w})$ are simple (i.e., $p = 1$) then*

$$a_{\boldsymbol{r}} = \left(\frac{1}{2\pi i}\right)^{d-1} \int_{\mathbf{T}(\boldsymbol{w}^\circ)} (\boldsymbol{z}^\circ)^{-\boldsymbol{r}^\circ} g(\boldsymbol{z}^\circ)^{-r_d} \Psi(\boldsymbol{z}^\circ) \frac{d\boldsymbol{z}^\circ}{\boldsymbol{z}^\circ},$$

*where $\Psi$ is given by* (9.13).

*Proof* This time we may take $C_1$ to be the circle of radius of $\rho - \delta$ and $C_2$ to be the circle of radius $\rho + \delta$ for any $\delta \in (0, \rho)$. The inner integral will be the sum of simple residues at points $g(\boldsymbol{z}^\circ)$ for any $\boldsymbol{z}^\circ$ and the proof is completed the same way as Theorem 9.17. □

In this case dimension is reduced by one without localizing. The localization occurs when we apply the multivariate saddle point results of Chapter 5, which implies that this $(d-1)$-dimensional integral is determined by the behavior of $g$ and $\Psi$ near the critical points on $T(\boldsymbol{w})$.

**Corollary 9.22.** *Suppose $\boldsymbol{w}$ satisfies all of the hypotheses of Theorem 9.5 except that instead of $\boldsymbol{w}$ being finitely minimal, $Q$ satisfies the torality hypothesis on $\mathbf{T}(\boldsymbol{w})$. Then the conclusions of Theorem 9.5 still hold.*

## 9.2 The method of residue forms

In this section we use the homological framework of previous chapters, together with the appendices, to prove Theorem 9.12. For convenience, we begin by naming the minimality property assumed in Theorem 9.12.

**Definition 9.23** (finite criticality)**.** We say $Q$ is ***finitely critical*** on the torus $\mathbf{T}(\boldsymbol{w})$ (in the direction $\hat{\boldsymbol{r}}$) if the intersection of $\mathcal{V}_Q$ with $\mathbf{T}(\boldsymbol{w})$ contains finitely many critical points of $Q$ in the direction $\hat{\boldsymbol{r}}$.

**Exercise 9.7.** For which directions $\hat{\boldsymbol{r}}$ (if any) does the function $Q(x, y) = (1 + x)(1 + y)$ satisfy finite criticality on the unit torus $\mathbf{T}(1, 1)$?

Suppose that $\boldsymbol{p}$ is a minimal point of $\mathcal{V}$ that is critical in direction $\hat{\boldsymbol{r}}$ and lies in the exponential torus $\mathbf{T}_e(\boldsymbol{x}) = \text{Relog}^{-1}(\boldsymbol{x})$ defined by some $\boldsymbol{x} \in \partial B$, where $B$ is a component of the complement of $\texttt{amoeba}(Q)$. Further assume that $\mathbf{T}_e(\boldsymbol{x}) \cap \mathcal{V}$ contains only finitely many critical points $\boldsymbol{p}_1, \ldots, \boldsymbol{p}_m$.

**Proposition 9.24** (stratified flow)**.** *For $\boldsymbol{x}' \in B$ arbitrarily close to $\boldsymbol{x}$, the torus $\mathbf{T}_e(\boldsymbol{x}')$ may be deformed in $\mathcal{M}$ so that it remains fixed in a neighborhood of each critical point $\boldsymbol{p}_j$ but moves to a height less than $-\hat{\boldsymbol{r}} \cdot \boldsymbol{x}$ outside of a larger neighborhood of each.*

*Proof* This is a consequence of Theorem 11.5, which uses *cones of hyperbolicity* to create a deformation based on Theorem 11.1. In the case that the points $\boldsymbol{p}_1, \ldots, \boldsymbol{p}_m$ are all smooth points, the cones and vectors can be constructed by the simpler and more explicit Theorem 11.9 and Corollary 11.10. □

We remark that because $\tilde{Q}$ is *hyperbolic* at all minimal points (see Proposition 11.26), the vector flow used in the proof of Proposition 9.24 can also be used to construct the general homotopy equivalence (C.3.1), giving the relative homology attachment groups up to points of height just below the minimal points. An important practical consequence is the following principle, stating that local integral formulae may be summed when finite criticality holds. It follows immediately from the deformation in Proposition 9.24.

**Theorem 9.25** (finite criticality implies sum of local contributions)**.** *Suppose that $\boldsymbol{w}$ is a minimal point satisfying finite criticality, with all critical points on $T(\boldsymbol{w})$ enumerated $\boldsymbol{p}_1, \ldots, \boldsymbol{p}_m$. If each of the $\boldsymbol{p}_j$ are nondegenerate contributing points and the Cauchy integral over a quasi-local cycle maximized near $\boldsymbol{p}_j$ has asymptotic expansion $\Phi_{\boldsymbol{p}_j}(\boldsymbol{r})$ then*

$$a_{\boldsymbol{r}} \approx \sum_{j=1}^{m} \Phi_{\boldsymbol{p}_j}(\boldsymbol{r}) + E(\boldsymbol{r}) \tag{9.17}$$

*where $E(\boldsymbol{r})$ grows exponentially slower than the common value of the $|\boldsymbol{p}_j^{-\boldsymbol{r}}|$.* □

Theorem 9.25 holds for general rational functions, not just those with smooth denominators, for more general definitions of *contributing points* that are discussed in later chapters.

https://doi.org/10.1017/9781108874144.014 Published online by Cambridge University Press

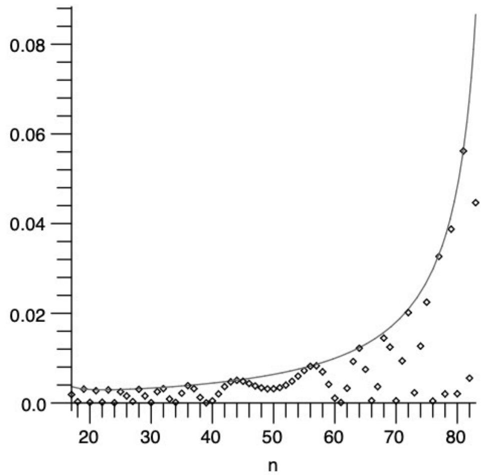


Figure 9.2 Spacetime generating function for a one-dimensional quantum walk.

**Exercise 9.8.** Let $Q(x, y) = 1 - cy(1 + x) - xy^2$, where $c \in (0, 1)$. The function $1/Q$ is the spacetime generating function for the simplest non-trivial one-dimensional quantum walk [BP07].

(a) Show that all singularities on the unit torus are minimal points.
(b) Show that the singularities on the unit torus are not finitely minimal.
(c) Show that for $|a - 1/2| < c/2$ and $\hat{\boldsymbol{r}} = \left[\frac{a}{a+1}, \frac{1}{a+1}\right]$ there are two critical points in the direction $\hat{\boldsymbol{r}}$ on the unit torus.
(d) Explain why (9.17) produces the picture in Figure 9.2 for the generating function $F(x, y) = 1/Q(x, y)$.

### 9.2.1 Theorem 9.12 via residue integrals

We are now ready to prove the *minimal point version* of the Main Theorem of Smooth ACSV.

*Proof of Theorem 9.12* Assume the hypotheses of Theorem 9.12 and let $B$ be the component of $\texttt{amoeba}(Q)^c$ corresponding to the convergent Laurent series under consideration. We use the homological constructions and terminology introduced in Appendix C. If $T = \mathbf{T}_e(\boldsymbol{x})$ for some $\boldsymbol{x} \in B$ and $T' = \mathbf{T}_e(\boldsymbol{x}')$ for some $\boldsymbol{x}' \in B'$, where $B'$ is one of the components of $\texttt{amoeba}(Q)^c$ on which $h_{\hat{\boldsymbol{r}}}$

https://doi.org/10.1017/9781108874144.014 Published online by Cambridge University Press

is not bounded from below (whose existence is guaranteed by Theorem 6.29), then the intersection class $\mathbf{INT}(T, T')$ is represented by the intersection of $\mathcal{V}$ with any homotopy from $T$ to $T'$ intersecting $\mathcal{V}$ transversely. Choosing such a homotopy whose time-$t$ cross-sections are tori that expand with $t$ and go through $\boldsymbol{w}$, perhaps slightly perturbed to intersect $\mathcal{V}$ transversely, the class $\mathbf{INT}(T, T')$ can be represented by a smooth $(d-1)$-chain $\gamma$ on $\mathcal{V}$ on which $h_{\hat{\boldsymbol{r}}}$ reaches its (not necessarily unique) maximum at $\boldsymbol{w}$. The Cauchy integral formula and the residue theorems from Chapter C imply

$$\begin{aligned} a_{\boldsymbol{r}} &= \frac{1}{(2\pi i)^d} \int_T F(\boldsymbol{z}) \boldsymbol{z}^{-\boldsymbol{r}-\boldsymbol{1}} \, d\boldsymbol{z} \\ &= \frac{1}{(2\pi i)^{d-1}} \int_\gamma \operatorname{Res}(F(\boldsymbol{z}) \boldsymbol{z}^{-\boldsymbol{r}-\boldsymbol{1}} \, d\boldsymbol{z}) + \frac{1}{(2\pi i)^{d-1}} \int_{T'} F(\boldsymbol{z}) \boldsymbol{z}^{-\boldsymbol{r}-\boldsymbol{1}} \, d\boldsymbol{z} \\ &= \frac{1}{(2\pi i)^{d-1}} \int_\gamma \operatorname{Res}(F(\boldsymbol{z}) \boldsymbol{z}^{-\boldsymbol{r}-\boldsymbol{1}} \, d\boldsymbol{z}). \end{aligned} \tag{9.18}$$

Assume first that $Q$ is square-free and $r_d > 0$, so that (C.2.1) in Proposition C.8 implies

$$a_{\boldsymbol{r}} = \frac{e^{-h_{\boldsymbol{r}}(\boldsymbol{w})}}{(2\pi i)^{d-1}} \int_\gamma e^{-\lambda \phi(\boldsymbol{z})} \frac{P(\boldsymbol{z})}{Q_{z_d}(\boldsymbol{z}) \prod_{j=1}^d z_j} \, d\boldsymbol{z}^\circ$$

with $\lambda = r_d$. Applying Theorem 5.3 with a generic triangulation of $C = \gamma$ gives an asymptotic expansion of $a_{\boldsymbol{r}}$ which, after the change of variables $z_j = w_j e^{i\theta_j}$ and algebraic simplification, gives the expression for $\Phi_{\boldsymbol{w}}$ in (9.2). Note that the Hessian determinant of $h_{\hat{\boldsymbol{r}}}$ on $\mathcal{V}$ with respect to the $\theta_j$ variables equals the Hessian determinant with respect to the $z_j$ variables multiplied by the Jacobian for the change of variables because the gradient of $h_{\hat{\boldsymbol{r}}}$ restricted to $\mathcal{V}$ vanishes at $\boldsymbol{w}$.

This completes the proof of Theorem 9.12 in the case that $p = 1$ and $r_d > 0$. The derivation for $p > 1$ is similar, with Lemma C.13 describing the residue and leading to (9.4). Likewise, accounting for the sign change in $\lambda = -r_d$ when $r_d < 0$ produces the sign factors in (9.4). □

### 9.2.2 Homological decompositions

Our results above help us prove that there is at most one torus containing smooth nondegenerate contributing points. A ***minimal torus*** with respect to a component $B$ and direction $\hat{\boldsymbol{r}}$ is a torus $\mathbf{T}_e(\boldsymbol{x})$ for some $\boldsymbol{x} \in \partial B$ minimizing $\hat{\boldsymbol{r}} \cdot \boldsymbol{x}$ on $\overline{B}$, containing at least one point $\boldsymbol{w} = \exp(\boldsymbol{x} + i\boldsymbol{y})$ that is critical in direction $\hat{\boldsymbol{r}}$.

**Proposition 9.26.** *Let $F(\boldsymbol{z}) = P(\boldsymbol{z})/Q(\boldsymbol{z})$ be the ratio of coprime polynomials $P$ and $Q$. Fix a direction $\hat{\boldsymbol{r}}$, a component $B$ of the complement of* $\mathtt{amoeba}(Q)$ *on which $h_{\hat{\boldsymbol{r}}}$ is bounded from below, and a component $B'$ on which $h_{\hat{\boldsymbol{r}}}$ is not bounded from below.*

*(i) There is at most one minimal torus with respect to $B$ and $\hat{\boldsymbol{r}}$ satisfying finite criticality and on which each critical point is smooth, contributing, and nondegenerate.*

*(ii) Let $T = \mathbf{T}_{\mathrm{e}}(\boldsymbol{x})$ for some $\boldsymbol{x} \in B$ and let $T' = \mathbf{T}_{\mathrm{e}}(\boldsymbol{x}')$ for some $\boldsymbol{x}' \in B'$. Given the existence of the torus described in $(i)$, the projection of $\mathbf{INT}(T, T')$ to the relative homology group $H_{d-1}(\mathcal{V}_*, \mathcal{V}_{\le c-\varepsilon})$, for sufficiently small $\varepsilon > 0$ and $c = -\hat{\boldsymbol{r}} \cdot \boldsymbol{x}$, equals $\sum_{\boldsymbol{z} \in \mathbf{W}} \gamma_{\boldsymbol{z}}$, where the cycle $\gamma_{\boldsymbol{z}}$ is a generator for the cyclic local homology group $H_{d-1}(\mathcal{V}_*^{\boldsymbol{z},\mathrm{loc}})$.*

*(iii) The projection of $[T]$ to $(\mathcal{M}, \mathcal{M}_{\le c-\varepsilon})$ is equal to $\sum_{\boldsymbol{z} \in \mathbf{W}} \mathtt{o}\gamma_{\boldsymbol{z}}$, where $\gamma_{\boldsymbol{z}}$ is a generator of the cyclic group $H_{d-1}\left(\mathcal{V}_*^{\boldsymbol{z},\mathrm{loc}}\right)$.*

*Proof* To prove $(i)$, suppose there are two such tori $\mathbf{T}_{\mathrm{e}}(\boldsymbol{x})$ and $\mathbf{T}_{\mathrm{e}}(\boldsymbol{x}')$. Applying Theorems 9.12 and 9.25 to the rational function $\tilde{F}(\boldsymbol{z}) = 1/\tilde{Q}(\boldsymbol{z})$ at the points in each torus gives two, necessarily equal, asymptotic series estimating the coefficients $\{\tilde{a}_{\boldsymbol{r}}\}$ uniformly as $|\boldsymbol{r}| \to \infty$ with $\boldsymbol{r}/|\boldsymbol{r}|$ remaining in some neighborhood $\mathcal{R}$ of $\hat{\boldsymbol{r}}$ (we replace $P$ by 1 and $Q$ by its square-free part as this does not change the minimal tori or our nondegeneracy assumptions, but simplifies the asymptotic formulae). In particular, the leading term of each expansion $\Phi_{\boldsymbol{w}}(\boldsymbol{r})$ in (9.4) has the form $C(\boldsymbol{w}) \exp(-\boldsymbol{r} \cdot \boldsymbol{x}) \exp(-i\boldsymbol{r} \cdot \boldsymbol{y}) r_d^{(1-d)/2}$ with $C$ nonvanishing. Summing the contributions of the finitely many points on $\mathbf{T}_{\mathrm{e}}(\boldsymbol{x})$ (respectively $\mathbf{T}_{\mathrm{e}}(\boldsymbol{x}')$) gives a function of $\boldsymbol{r}$ that is nonvanishing at least on some finite-index sublattice of $\mathbb{Z}^d$. Furthermore, the terms given by the elements of $\mathbf{T}_{\mathrm{e}}(\boldsymbol{x})$ and the elements of $\mathbf{T}_{\mathrm{e}}(\boldsymbol{x}')$ differ from each other in exponential growth, because $-\boldsymbol{x} \cdot \boldsymbol{r}$ and $-\boldsymbol{x}' \cdot \boldsymbol{r}$ disagree on $\mathcal{R}$ except possibly for a set of codimension 1. This contradicts the fact that both expansions represent asymptotics for the same sequences, so two such tori cannot exist.

To prove $(ii)$, the deformation used to prove Theorem 5.3 shows that the intersection cycle may be deformed to a sum of elements of local homology groups. None of these can be zero because there is a term corresponding to each in (9.8). Similarly, each is a relative homology generator: this can be seen from the deformation, but an easier argument is that the corresponding term $\Phi_{\boldsymbol{w}}(\boldsymbol{r})$ is, up to sign, the integral obtained from a small $(d-1)$-patch and we know the local homology generator is a $(d-1)$-ball modulo its boundary (see, for example, Theorem C.38).

Conclusion $(iii)$ can be argued similarly to $(ii)$, using the stratified description of attachments from Theorem D.25 in place of Theorem C.38. Alterna-

https://doi.org/10.1017/9781108874144.014 Published online by Cambridge University Press

tively, the Thom isomorphism (Theorem C.2) says that $\circ$ induces an injection from $H_{d-1}(\mathcal{V}_*)$ to $H_d(\mathbb{C}^d_* \setminus \mathcal{V})$. Being functorial, it commutes with $\pi_*$ where $\pi : \mathcal{V}_* \to (\mathcal{V}_*, \mathcal{V}_{\leq c-\varepsilon})$ is projection. The Thom isomorphism carries $\mathbf{INT}(T, T')$ to $T - T'$, which is equal to $T$ in $H_d(\mathcal{V}_*, \mathcal{V}_{\leq c-\varepsilon})$, proving (*iii*). □

We remark that it is possible to have a minimal smooth contributing point $\boldsymbol{p}$ in the direction $\hat{\boldsymbol{r}}$, and another smooth critical (but not contributing) point $\boldsymbol{p}'$ in the direction $\hat{\boldsymbol{r}}$ *that is not minimal* but has the same height as $\boldsymbol{p}$.

## 9.3 Smooth bivariate functions

This section further explores bivariate rational functions, for which we can be more explicit and give stronger results.

### 9.3.1 Smooth bivariate power series

We first present a complete algorithm for bivariate power series that finds all smooth contributing critical points, without any assumption of minimality, following the techniques of [DeV11; DvdHP11].

**Assumption 9.1.** *In this section we always assume that $\mathcal{V}$ is smooth and $Q$ is square-free, so that for every $(x, y) \in \mathcal{V}$, at least one of $Q_x(x, y)$ and $Q_y(x, y)$ is non-zero, and that the set of critical points is finite. If $Q$ is not square-free then our arguments characterizing the singularities that determine asymptotics still hold when $Q$ is replaced by its square-free part.*

In any number of variables, a potential program to determine asymptotics is the following.

1. Explicitly compute a cycle representing the intersection class.
2. Try to push the cycle below each critical point, starting at the highest.
3. When it is not possible to push past a point, describe the local cycle that is ‘snagged’ on the critical point.
4. Check whether this is a quasi-local cycle of the form we have already described and, if so, read off the estimate from saddle point asymptotics.

This program is not generally effective because the step of ‘pushing the cycle down’ is not algorithmic, which is why we use the framework of stratified Morse theory. However, an exception occurs when $d = 2$, since the cycle $C$ has codimension 1 in $\mathcal{V}$ and thus, up to a time change, there is only one way for it to flow downward.

https://doi.org/10.1017/9781108874144.014 Published online by Cambridge University Press

Fix a direction $\hat{\mathbf{r}} = (\hat{r}, \hat{s})$ with $\hat{r}$ and $\hat{s}$ positive (otherwise all series coefficients in this direction are zero, or given by a univariate rational function, since we consider the power series expansion of $F$). Because $Q$ does not vanish at the origin, there exists some $\varepsilon > 0$ such that $\mathcal{V} = \mathcal{V}_Q$ does not intersect the set $\{(x,y): |x| \le \varepsilon, |y| \le \varepsilon\}$. Now, for any $c \in \mathbb{R}$ if the height $h(x,y) = -\hat{r}\log|x| - \hat{s}\log|y|$ of a point $(x,y)$ is at least $c$ then either $|x| \le e^{-c}$ or $|y| \le e^{-c}$. Taking $c \ge \log(1/\varepsilon)$ thus shows that no connected component of $\mathcal{V}^{\ge c}$ contains both points with $|x| \le \varepsilon$ and points with $|y| \le \varepsilon$.

On the other hand, for sufficiently large $c$ every connected component of $\mathcal{V}^{\ge c}$ contains points with arbitrarily large height, and hence points with either $|x| \le \varepsilon$ or $|y| \le \varepsilon$. Thus, we may decompose $\mathcal{V}^{\ge c}$ for sufficiently large $c$ into a disjoint union $X^{\ge c} \cup Y^{\ge c}$, where $X^{\ge c}$ is the union of connected components containing points with arbitrarily small $x$-coordinates and $Y^{\ge c}$ is the union of connected components containing points with arbitrarily small $y$-coordinates. Puiseux's Theorem states that in a sufficiently small neighborhood of the origin in $x$, with a ray from the origin removed to account for branch cuts, every branch $y(x)$ of $Q(x,y) = 0$ has a representation

$$y(x) = \sum_{j \ge j_0} c_j x^{j/k}$$

for a fixed branch of the $k$th root, where $j_0 \in \mathbb{Z}$ and $k$ is a positive integer (and analogous representations for the branches of $x$ in terms of $y$ also hold). By Rouché's Theorem, projection of such a connected component to its $x$-value is diffeomorphic as a covering to the projection of the graph of $y^k = Cx^j$ for some constant $C$, such a covering space being diffeomorphic to a punctured disk. Thus, for any sufficiently large $c$, the connected components of $X^{\ge c}$ and $Y^{\ge c}$ are diffeomorphic to disjoint open disks with their origins removed. The values of $c$ such that this decomposition holds form an interval $[c_{xy}, \infty)$ for some $c_{xy} \in \mathbb{R}$.

**Critical points at infinity**

Puiseux's Theorem also helps characterize critical points at infinity. In particular, any branch $y(x)$ of $Q(x,y) = 0$ near the origin $x = 0$ satisfies

$$y(x) = Cx^{\alpha}(1 + o(1))$$

for some $C \in \mathbb{C}$ and $\alpha \in \mathbb{Q}$, and any branch $x(y)$ near the origin $y = 0$ satisfies

$$x(y) = C'y^{\beta}(1 + o(1))$$

for some $C' \in \mathbb{C}$ and $\beta \in \mathbb{Q}$. If $F(x,y)$ has a CPAI in the direction $\hat{\mathbf{r}}$ then either $\alpha = -\frac{\hat{r}}{\hat{s}}$ for some branch $y(x)$ or $\beta = -\frac{\hat{s}}{\hat{r}}$ for some branch $x(y)$. We thus make the following assumption to rule out the existence of CPAI.

**Assumption 9.2** (No CPAI)**.** *For any branch* $y(x) = Cx^\alpha(1+o(1))$ *of* $Q(x,y) = 0$ *as* $x \to 0$ *we have* $\alpha \neq -\frac{\hat{r}}{\hat{s}}$ *and for any branch* $x(y) = C'y^\beta(1+o(1))$ *of* $Q(x,y) = 0$ *as* $y \to 0$ *we have* $\beta \neq -\frac{\hat{s}}{\hat{r}}$.

When Assumption 9.2 holds we can be very explicit about the behavior of the height function near the coordinate axes.

**Lemma 9.27.** *Assume there are no CPAI. For any sufficiently small* $\varepsilon > 0$, *fixed* $\theta \in [-\pi,\pi]$, *and branch* $y(x)$ *of* $Q(x,y) = 0$ *near* $x = 0$, *the parametrized height function*

$$h_\theta(t) = h\left(te^{i\theta}, y\left(te^{i\theta}\right)\right)$$

*is monotonic for* $t \in [0,\varepsilon]$. *Furthermore, if* $y(x) \sim Cx^\alpha$ *as* $x \to 0$ *then*

$$\lim_{t\to 0^+} h_\theta(t) = \begin{cases} \infty & \text{if } \alpha > -\hat{r}/\hat{s} \\ -\infty & \text{if } \alpha < -\hat{r}/\hat{s} \end{cases}.$$

*Proof* Puiseux's theorem implies we can always find $\alpha \in \mathbb{Q}, C \in \mathbb{C}$, and a function $\phi$ with $\phi(x)$ and $x\phi'(x)$ in $o(1)$ such that $y(x) = Cx^\alpha(1+\phi(x))$ as $x \to 0$. The height function is the real part of $H(x,y) = -\hat{r}\log x - \hat{s}\log y$, so

$$\frac{d}{dt}h_\theta(t) = \cos(\theta)\mathrm{Re}\left[H_x(x,y(x))\right] - \sin(\theta)\mathrm{Im}\left[H_x(x,y(x))\right],$$

where

$$H_x(x,y(x)) = \frac{-\hat{r}-\hat{s}\alpha}{x} - \frac{\phi'(x)}{1+\phi(x)} \sim \frac{-\hat{r}-\hat{s}\alpha}{x}.$$

Thus

$$\frac{d}{dt}h_\theta(t) \sim \frac{-\hat{r}-\hat{s}\alpha}{|x|},$$

which is strictly positive or strictly negative under Assumption 9.2. Finally, we note

$$h_\theta(t) \sim \log\left(Ct^{-\hat{r}-\hat{s}\alpha}\right)$$

for $t$ sufficiently small, giving the stated asymptotic behavior. □

**Corollary 9.28.** *Under Assumption 9.2 the connected components of* $X^{\geq c}$ *are diffeomorphic to disjoint open disks with their origins removed, corresponding to the branches* $y(x) \sim Cx^\alpha$ *of* $Q(x,y) = 0$ *as* $x \to 0$ *with* $-\hat{r}/\hat{s} < \alpha \leq 0$.

### Intersection cycles and flows

Fixing $|x|$ small and expanding $|y|$ gives a homotopy that (up to minor perturbation) intersects $\mathcal{V}$ transversely. In particular, the intersection cycle $C$ created from this operation contains a positively oriented circle around the removed origin from each of the punctured disks in $X^{\geq c}$ for $c$ sufficiently large. As usual, we get a residue integral expression

$$a_{r,s} = \frac{1}{2\pi i}\int_C \operatorname{Res}\left(\frac{P(x,y)}{Q(x,y)}x^{-r-1}y^{-s-1}dx\wedge dy\right)$$

when $P$ and $Q$ are polynomials. More generally, when $P$ is an analytic function over appropriate regions of $\mathbb{C}^d$ we get

$$a_{r,s} = \frac{1}{2\pi i}\int_C \operatorname{Res}\left(\frac{P(x,y)}{Q(x,y)}x^{-r-1}y^{-s-1}dx\wedge dy\right) + O(\delta^{r+s})$$

as $r, s \to \infty$, for any $\delta > 0$.

As we have already seen multiple times, in the absence of CPAI the topology of $\mathcal{V}^{\geq c}$ cannot change with $c$ except at critical values. Because we work in two dimensions, we can be very explicit about the change in topology as $c$ passes through a critical value.

**Definition 9.29.** Suppose $\boldsymbol{\sigma} = (x_0, y_0)$ is a critical point where $Q_x(\boldsymbol{\sigma}) \neq 0$, so that we can parametrize $y = y(x)$ in a neighborhood of $\boldsymbol{\sigma}$ in $\mathcal{V}$. The ***degree of degeneracy*** of $Q$ at $\boldsymbol{\sigma}$ is the integer $k$ such that there is a series expansion

$$h(x, y(x)) = h(\boldsymbol{\sigma}) + \operatorname{Re}\left[\sum_{j\geq k} c_j(x-x_0)^j\right]$$

in a neighborhood of $x_0$ with $c_k \neq 0$. Because $\boldsymbol{\sigma}$ is a critical point of the height function $h$, the degree of degeneracy is always at least 2, and $\boldsymbol{\sigma}$ is a nondegenerate critical point precisely when the degree of degeneracy is equal to 2. Because $\hat{\mathbf{r}}$ has no zero coordinate and $\boldsymbol{\sigma}$ is a critical point, $Q_y(\boldsymbol{\sigma}) \neq 0$ and the degree of degeneracy is the same parametrizing by $y$ instead of $x$.

If $\boldsymbol{\sigma} = (x_0, y_0)$ is a critical point with degree of degeneracy $k$ then we can substitute $y = y(x)$ and expand $H(x,y) = -\hat{r}\log x - \hat{s}\log y$ near $x_0$ to obtain

$$H(x, y(x)) = C + (x-x_0)^k g(x)$$

for some $C \in \mathbb{C}$ and analytic function $g$ with $g(x_0) \neq 0$. In particular, if $w = (x-x_0)g(x)^{1/k}$ then $(dw/dx)(x_0) \neq 0$ and we can parametrize the height function $h$ in the local coordinate $w$ near $\boldsymbol{\sigma}$ as

$$h(x(w), y(x(w))) = \operatorname{Re}\left[H(x(w), y(x(w)))\right] = h(\boldsymbol{\sigma}) + \operatorname{Re}\left[w^k\right].$$

https://doi.org/10.1017/9781108874144.014 Published online by Cambridge University Press

Thus, near $\boldsymbol{\sigma}$ the set $\mathcal{V}$ contains $k$ disjoint *ascent regions*, where $h$ increases while moving towards $\boldsymbol{\sigma}$, which alternate with $k$ disjoint *descent regions*, where $h$ decreases while moving towards $\boldsymbol{\sigma}$; this is illustrated in Figure 9.5 below.

**Definition 9.30.** Let $c_{xy} \in [-\infty, \infty)$ be the infimum of all values $c$ such that $X^{>c} \cap Y^{>c} = \emptyset$ (which is also the smallest value $c$ such that $X^{>c}$ and $Y^{>c}$ are well-defined). If $c_{xy} = -\infty$ then let $\mathbf{W} = \emptyset$, otherwise let $\mathbf{W}$ be the nonempty set of critical points $\boldsymbol{\sigma}$ such that $h(\boldsymbol{\sigma}) = c_{xy}$ and, for any sufficiently small neighborhood $U$ of $\boldsymbol{\sigma}$ in $\mathcal{V}$, the sets $U \cap X^{>c_{xy}}$ and $U \cap Y^{>c_{xy}}$ are nonempty.

Our choice of the notation $\mathbf{W}$ comes from the following result.

**Theorem 9.31.** *Suppose Assumptions 9.1 and 9.2 hold. If* $\mathbf{W}$ *is empty then the intersection cycle* $C$ *is in the same homology class as a cycle with maximum height* $-m$ *for all sufficiently large* $m \in \mathbb{R}$ *(it can be pushed down forever). If* $\mathbf{W}$ *is nonempty then* $C$ *is in the same homology class as a cycle* $\kappa$ *such that*

*(i) The points of* $\kappa$ *with maximum height are precisely the points of* $\mathbf{W}$.

*(ii) For* $\boldsymbol{\sigma} \in \mathbf{W}$ *and a sufficiently small neighborhood* $U$ *of* $\boldsymbol{\sigma}$ *in* $\mathcal{V}$, *if* $A_0, \ldots, A_{k-1}$ *and* $D_0, \ldots, D_{k-1}$ *denote the ascent and descent regions of* $\kappa \cap U$ *enumerated counterclockwise such that* $D_j$ *lies between* $A_j$ *and* $A_{j+1 \bmod k}$ *then*

$$\kappa \cap U = \sum_{j=0}^{k-1} \Big[X(j+1) - X(j)\Big]\gamma_j,$$

*where each* $\gamma_j$ *is a curve traveling downward in* $D_j$ *starting at* $\boldsymbol{\sigma}$ *and*

$$X(j) = \begin{cases} 1 & \text{if } A_{j \bmod k} \subset X^{>c_{xy}} \\ 0 & \text{if } A_{j \bmod k} \subset Y^{>c_{xy}} \end{cases}.$$

*In particular,* $\kappa \cap U$ *projects to a non-trivial cycle in the relative homology group* $H_1(U, U \cap \mathcal{V}^{\leq c_{xy}-\varepsilon})$ *for any* $\varepsilon > 0$ *sufficiently small (so the intersection cycle gets stuck at height* $c_{xy}$*).*

*Proof* Let $M \in \mathbb{R}$ be larger than all critical values of $h$. Then $C$ is homologous to closed curves in each component of $X^{\geq M}$, and in fact it is homologous to the boundary $\partial X^{\geq M}$. First, we show that we can push down the intersection cycle until arriving at $c_{xy}$. The topology of $\mathcal{V}^{\geq c}$ only changes at critical values $c$, so let $\sigma$ be a critical value in $(c_{xy}, M]$ and suppose that $\boldsymbol{\sigma}$ is the only critical point with $h(\boldsymbol{\sigma}) = \sigma$.

Figure 9.3 shows $\mathcal{V}^{\geq c}$ (shaded) for three values of $c$ when the degree of degeneracy of $\boldsymbol{\sigma}$ is $k = 2$ and a circle enclosing a region where the parametrization $h = \sigma + \mathrm{Re}[w^k]$ holds (higher degrees of degeneracy are similar, just with

https://doi.org/10.1017/9781108874144.014 Published online by Cambridge University Press

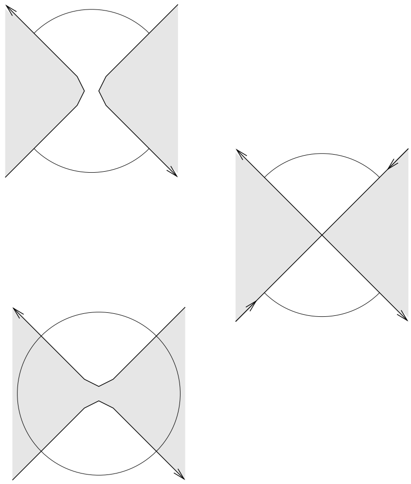

Figure 9.3 $\mathcal{V}^{\geq c}$ and its boundary for three values of $c$.

more components). In the top diagram $c > \sigma$, in the middle diagram $c = \sigma$, and in the bottom $c < \sigma$, with the arrows showing the orientation of $\partial\mathcal{V}^{\geq c}$ inherited from the complex structure of $\mathcal{V}$.

Consider the first picture where $c > \sigma$. Because $c > c_{xy}$ each of the $k$ shaded regions is in $X^{\geq c}$ or $Y^{\geq c}$, but not both. In fact, since $\sigma > c_{xy}$ this persists in the limit as $c \downarrow \sigma$, so either all $k$ regions are in $Y^{\geq c}$ or all $k$ regions are in $X^{\geq c}$. In the first case $\partial X^{\geq c}$ does not contain any critical points of $h$ on $\mathcal{V}$ with height in an interval $(\sigma - 2\varepsilon, \sigma + 2\varepsilon)$, so the first Morse Lemma implies $\partial X^{\geq \sigma+\varepsilon}$ is homotopic to $\partial X^{\geq \sigma-\varepsilon}$ as desired. In the latter case, the difference between $\partial\mathcal{V}^{\geq \sigma+\varepsilon}$ and $\partial\mathcal{V}^{\geq \sigma-\varepsilon}$ is a boundary $\partial B$ (see Figure 9.4, or Figure 9.5 below) so these sets are still homologous. In fact, one can show they are still homotopic.

Thus, we can push the intersection cycle below any critical value above $c_{xy}$ that has a single corresponding critical point, and the same argument holds generally by working locally around each critical point of fixed height larger than $c_{xy}$. In particular, if $\mathbf{W}$ is empty then we can push the intersection cycle down to arbitrarily low height.

It remains only to show that the intersection cycle can be represented by the stated cycle $\kappa$. Just as in Figure 9.3, the connected components of $\partial X^{\geq c_{xy}+\varepsilon}$ will contain curves moving through a descent region of $\mathcal{V}$ near $\boldsymbol{\sigma}$, crossing over an ascent region, then going back out through an adjacent descent region. However, unlike for critical points at higher height where all ascent regions are

https://doi.org/10.1017/9781108874144.014 Published online by Cambridge University Press

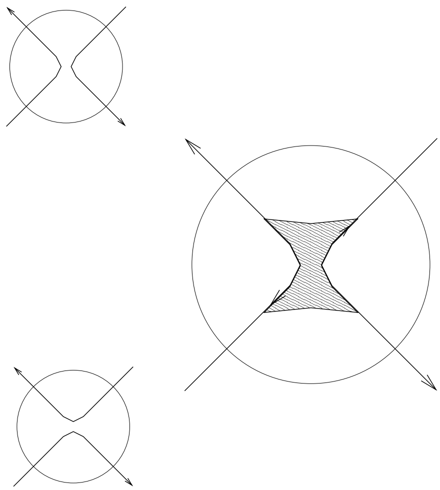

Figure 9.4 $\partial\mathcal{V}^{\geq\sigma+\varepsilon}$ and $\partial\mathcal{V}^{\geq\sigma-\varepsilon}$ differ locally by a boundary.

covered or none were, in this case the curves will only cross the ascent regions containing points of $X^{>c_{xy}}$; see Figure 9.5.

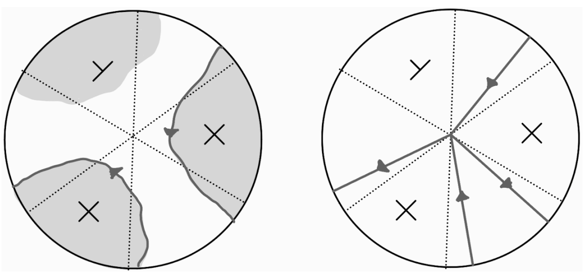

Figure 9.5 *Left:* Plot of $\mathcal{V}$ near a critical point with degree of degeneracy $k = 3$, where $\mathcal{V}^{>c_{xy}}$ contains two ascent regions with points in $X^{>c_{xy}}$ and one region with points in $Y^{>c_{xy}}$. The set $\mathcal{V}^{>c_{xy}+\varepsilon}$ is colored gray and the part of $\partial X^{\geq c_{xy}+\varepsilon}$ in view is drawn. *Right:* Straightening out the connected components of $\partial X^{\geq c_{xy}+\varepsilon}$ near this critical point gives the stated curves $\gamma_j$.

The connected components of $\partial X^{\geq c_{xy}+\varepsilon}$ can be straightened into rays $\gamma_j$ (in terms of the local coordinate $w$) that stay in each descending region adjacent to an ascending region containing points of $X^{>c_{xy}}$. If the descending region is between ascending components containing points of $Y^{>c_{xy}}$ and $X^{>c_{xy}}$, working counterclockwise, then $\gamma_j$ will start at the critical point and move down the descending region. Conversely, if the descending region is between ascending components containing points of $X^{>c_{xy}}$ and $Y^{>c_{xy}}$, working counterclockwise, then $\gamma_j$ will move up the descending region to peak at the critical point. Descending regions between two ascending regions both containing points of $X^{>c_{xy}}$ have $\gamma_j$ twice with opposite orientations, which can be joined and pushed to lower height. Descending regions between two ascending regions both containing points of $Y^{>c_{xy}}$ are not touched by the intersection cycle. Taking these sign considerations into account gives the stated formula for $\kappa$. □

Theorem 9.31 immediately gives an algorithm for the bivariate case.

**Algorithm 3:** Determination of **W** in the smooth, bivariate case.

**Input:** Bivariate rational function $F(x, y)$ and direction $(r, s)$.
**Output:** Set of critical points **W** determining coefficient asymptotics of $F$ in the $(r, s)$ direction.

1 Verify that Assumptions 9.1 and 9.2 hold using Gröbner bases and Puiseux expansions
2 List the critical value in order of decreasing height
3 Set the provisional value of $c_{xy}$ to the highest critical value
4 For each critical point at height $c_{xy}$ do
 (a) Compute the order $k$ of the critical point
 (b) Follow each of the $k$ ascent paths until it is clear whether the $x$-coordinate or the $y$-coordinate goes to zero
 (c) Add the point to the set **W** if and only if at least one of the $k$ paths has $x$-coordinate going to zero and at least one of the $k$ paths has $y$-coordinate going to zero
5 If **W** is nonempty then terminate and output $c_{xy}$ and **W**
6 Else, if $c_{xy}$ is not the least critical value then replace $c_{xy}$ by the next lower critical value and go to step 4
7 Else, if no critical values remain then $c_{xy} = -\infty$, **W** is empty, and the asymptotics decay super-exponentially

The doctoral dissertation [DeV11] discusses how to turn this breakdown into effective steps, and [MS22] give an implementation in Sage using interval arithmetic. The trickiest part is Step 4b. Ascent paths could conceivably get caught in a trap, approaching a critical point rather than continuing to height $+\infty$. However, this is a higher critical point, hence already known to be in an $x$- or $y$-component. Therefore, one only needs to know a radius $\varepsilon$ for each higher critical point $\boldsymbol{p}$ such $|\boldsymbol{w} - \boldsymbol{p}| < \varepsilon$ implies $\boldsymbol{w}$ is in the same component as $\boldsymbol{p}$, which can be done with interval arithmetic. We conclude this section with an example of the evaluation of the intersection class for a particular smooth bivariate generating function whose analysis first appeared in [DeV10].

**Example 9.32** (bi-colored supertrees)**.** A ***bi-colored supertree*** [FS09, Example VI.10] is a planar binary tree with each node replaced by a bi-colored rooted planar binary tree. The class of bi-colored supertrees is counted by the main diagonal of the bivariate function

$$F(x, y) = \frac{P(x, y)}{Q(x, y)} = \frac{2x^2y(2x^5y^2 - 3x^3y + x + 2x^2y - 1)}{x^5y^2 + 2x^2y - 2x^3y + 4y + x - 2},$$

and we give asymptotics following the algorithm above.

First, we note that there is one branch $y(x) \sim (-4)x^{-5}$ of $y$ as $x \to 0$ and four branches $x(y)$ of $x$ as $y \to 0$, two of which satisfy $x(y) \sim y^{-1/2}$ and two of which have $x(y) \sim -y^{-1/2}$. In particular, there are no critical points at infinity in the main diagonal direction $(r, s) = (1, 1)$. A quick Gröbner basis computation further verifies that the system

$$Q(x, y) = Q_x(x, y) = Q_y(x, y) = 0$$

has no solution, and the smooth critical point system

$$Q(x, y) = xQ_x(x, y) - yQ_y(x, y) = 0$$

has three solutions

$$\left(1 - \sqrt{5}, \frac{3 + \sqrt{5}}{16}\right), \quad \left(2, \frac{1}{8}\right), \quad \left(1 + \sqrt{5}, \frac{3 - \sqrt{5}}{16}\right),$$

listed here in order of decreasing height under $h_{1/2,1/2}$.

The highest critical point is nondegenerate, meaning $\mathcal{V}$ locally has two ascent paths. Following both ascent paths using, for instance, the Sage package of [MS22] shows that both contains points arbitrarily close to the $x$-axis, so the intersection cycle can be pushed lower. In this case we could also simply observe that the highest critical point cannot contribute to the asymptotics because the coordinates are real and of opposite sign. The factor $x^{-n}y^{-n}$ in the asymptotic formula for $a_{n,n}$ would then force the signs to alternate on the diagonal, whereas we know the diagonal terms to be positive.

Continuing to the next-highest point we consider the point $(2, 1/8)$. This point has degree of degeneracy four, of which three climb to the $x$-axis and one climbs to the $y$-axis. In particular, the point $(2, 1/8)$ determines dominant diagonal asymptotics and, using the notation of Theorem 9.31, the intersection cycle is homologous to $\gamma = \gamma_j - \gamma_{j-1}$ where $j$ is the index of the region whose ascent region goes to the $y$-axis. Among the four descent regions, this path inhabits two consecutive ones, making a right-angle turn as it passes through the saddle.

Finally, we evaluate the univariate integral over this cycle. To compute the residue form in this example it is easiest to parametrize a neighborhood of $(2, 1/8)$ in $\mathcal{V}$ by the $x$-coordinate and use Proposition C.8 from Appendix C with $j = 2$ to see that

$$\omega = \operatorname{Res}\left(F(x,y)x^{-n-1}y^{-n-1}dx \wedge dy\right) = \frac{-P(x,y)}{xy(x)Q_y(x,y(x))}x^{-n}y(x)^{-n}\,dx.$$

Moving the origin to $x = 2$, equals

$$\frac{1}{2\pi i}\int_\gamma \omega = 4^n \int_\gamma A(x)e^{-n\phi(x)}\,dx$$

where the series expansions for $A$ and $\phi$ are given by

$$A(x) = -\frac{x^3}{8} - \frac{x^4}{16} + O(x^5)$$

$$\phi(x) = -\frac{x^4}{16} + O(x^6)\,.$$

Applying Theorem 4.1 to evaluate the integral on the segment $-\gamma_{j+1}$ using the parametrization $x = (i-1)t$ for $0 \le t \le \varepsilon$ gives a series for $\frac{1}{2\pi i}\int \omega$ that begins

$$4^n\left(\frac{-i}{4\pi}n^{-1} + \frac{(1+i)\sqrt{2}\Gamma(5/4)}{8\pi}n^{-5/4} + O(n^{-3/2})\right).$$

Similarly, on $\gamma_j$ we parametrize by $x = (-i-1)t$ and obtain the complex conjugate of the previous expansion,

$$4^n\left(\frac{i}{4\pi}n^{-1} + \frac{(1-i)\sqrt{2}\Gamma(5/4)}{8\pi}n^{-5/4} + O(n^{-3/2})\right).$$

When the two contributions are summed the first terms cancel and we are left with

$$a_{n,n} \sim \frac{4^n\sqrt{2}\Gamma(5/4)}{4\pi}\,n^{-5/4}\,.$$

◁

### 9.3.2 Laurent series

In this section we discuss what can be done when the hypotheses of Algorithm 3 are satisfied, except that the series in question is a Laurent series rather than an ordinary power series. We first revisit Algorithm 3 from a different point of view, involving intersection numbers of middle-dimensional cycles.

**Definition 9.33.** Let $X$ be a smooth, oriented real $2k$-manifold, and let $\gamma_1$ and $\gamma_2$ be two smooth, oriented $k$-cycles on $X$, intersecting transversely at finitely many points $\boldsymbol{x}_1, \ldots, \boldsymbol{x}_m$. The ***signed intersection number*** of $\gamma_1$ and $\gamma_2$ is the integer

$$\#(\gamma_1, \gamma_2) = \sum_{j=1}^{m} \operatorname{sgn}(\boldsymbol{x}_j),$$

where $\operatorname{sgn}(\boldsymbol{x}_j) = 1$ if the oriented bases $B_1$ and $B_2$ for the tangent spaces $T_p(\gamma_1)$ and $T_p(\gamma_2)$ form (in this order) a positively oriented basis for the tangent space $T_p(X)$, and $\operatorname{sgn}(\boldsymbol{x}_j) = -1$ otherwise.

The following construction can be found in [GP74] or [BJ82, pages 151–152].

**Proposition 9.34.** *Let $X$ be an oriented real manifold of dimension $2k$ and let $\alpha$ and $\beta$ be smooth oriented compact cycles of dimension $k$. Then generic perturbations of $\alpha$ and $\beta$ will intersect transversely in a finite number of points [GP74, Section 2.3], and the resulting signed intersection number does not depend on the generic perturbation. In fact, the signed intersection number is an invariant [GP74, Section 3.3] of the homology classes $[\alpha]$ and $[\beta]$ in $H_k(X)$.* □

Let $h$ be a (not necessarily proper) smooth Morse function on a complex $k$-manifold $X$ with finitely many critical points $\boldsymbol{x}_1, \ldots, \boldsymbol{x}_m$, listed in order of decreasing height $h(\boldsymbol{x}_1) \geq \cdots \geq h(\boldsymbol{x}_m)$, such that all critical points have middle index $k$. For each $j \leq m$, let $\gamma_j$ be a smooth cycle agreeing with the stable manifold of the (upward) gradient flow of $h$ in a neighborhood of $\boldsymbol{x}_j$ having $\boldsymbol{x}_j$ as its highest point. Similarly, let $\gamma^j$ be a smooth cycle agreeing with the unstable manifold of the gradient flow of $h$ in a neighborhood of $\boldsymbol{x}_j$ with $\boldsymbol{x}_j$ as its lowest point. The $\gamma_j$ are absolute cycles representing attachments in the Morse filtration at $\boldsymbol{x}_j$ (described in Appendix C). Similarly, the $\gamma^j$ are absolute cycles representing attachments in the reverse Morse filtration at $\boldsymbol{x}_j$, obtained by replacing $h$ by $-h$.

**Proposition 9.35.** *Let $L$ be the subspace of $H_k(X)$ generated over the complex numbers by $\{[\gamma_j] : j \leq m\}$ and let $L^*$ denote the dual space to $L$. Then $\{[\gamma^j] : j \leq m\}$ is a basis for $L^*$ and the signed intersection number $\#(\gamma_i, \gamma^j)$ is a nonsingular pairing whose representing matrix $M$ is upper triangular.*

*Proof* When $i = j$ the cycles $\gamma_i$ and $\gamma^j$ represent the stable and unstable manifolds of the gradient flow for a Morse function at the critical point $\boldsymbol{x}_j$. Morse functions are quadratically nondegenerate, therefore locally these intersect transversely at a single point, and they cannot intersect anywhere else due to the height restrictions. Hence the intersection number is $\pm 1$. When $i > j$ the height restrictions prevent $\gamma_i$ and $\gamma^j$ from intersecting at all, whence $M_{ij} = 0$, so $M$ is an upper triangular matrix with $\pm 1$ diagonal entries, and thus nonsingular. □

**Remark 9.36.** If $h(\boldsymbol{x}_j) = h(\boldsymbol{x}_{j+r})$ for $r \geq 1$ then again the height restrictions prevent $\gamma_i$ from intersecting $\gamma^\ell$ when $i$ and $\ell$ are distinct elements of $\{j, \ldots, j + r\}$, hence the only non-zero entries in the submatrix $M_{[j,j+r],[j,j+r]}$ are those on the diagonal.

Algorithm 3 may be understood in terms of this pairing, as we now sketch.

*Sketched alternative proof of correctness for Algorithm 3* Suppose that some component $B'$ of the complement of the amoeba of $Q(x, y)$ contains a ray with small $x$ coordinate that points up in the $y$ direction, let $T$ be the torus of integration for the bivariate Cauchy integral, with both $x$- and $y$-radii arbitrarily small, and let $\gamma$ be the intersection cycle $\mathbf{INT}(T, T')$, where the basepoint of $T'$ still has small $x$-coordinate but has sufficiently large $y$-coordinate to be in $B'$. Then $\gamma$ consists of small cycles around the points $(0, s)$, as $s$ ranges over the roots of $Q(0, y)$. Assuming these to be simple roots, the circles wind once about the origin.

The key is to interpret Steps 4(b-c) in Algorithm 3 using intersection numbers. Suppose $\boldsymbol{p}_j$ is a nondegenerate critical point reached by the algorithm, with corresponding ascent path $\gamma^j$. Steps 4(b-c) compute the intersection number of $\gamma$ with $\gamma^j$. If, among the two branches of $\gamma$, one goes to the $x$-axis and one goes to the $y$-axis, then $\gamma$ will intersect precisely one of the circles around a point $(0, s)$ and the intersection number will be $\pm 1$. If both branches go to the $x$-axis then the intersection number is zero because they cannot intersect any of the small circles around the points $(0, s)$. Furthermore, the intersection number depends only on the homology class of the intersection cycle $\gamma$ and, as shown in Corollary C.5 of Appendix C, the homology class of the intersection cycle obtained by keeping $|x|$ small and taking $|y|$ to infinity is the same as the intersection cycle obtained by keeping $|y|$ small and expanding $|x|$ to infinity. Interpreting the intersection cycle using this second construction shows that if both branches go to the $y$-axis then the intersection number is also zero.

The upshot is that in Step 4(c), the point $\boldsymbol{p}_j$ is added to $\mathbf{W}$ if and only if $\#(\gamma, \gamma^j) = \pm 1$ is non-zero. If any point at a given height is added, then all points at that height are added for which the intersection number of the ascent path with $\gamma$ is $\pm 1$ and no lower points are added. Inverting the dual basis shows that $\gamma - \sum_{i:\boldsymbol{p}_i \in \mathbf{W}} \pm \gamma_i$ is zero in $H_1(\mathcal{V}_*, \mathcal{V}_{<c_{xy}})$. □

We now return to the case of more general Laurent series. The difference

https://doi.org/10.1017/9781108874144.014 Published online by Cambridge University Press

between these and ordinary power series is that we can no longer count on the intersection cycle $\gamma$ to be the union of small circles around points of intersection of $\mathcal{V}$ with one of the coordinate axes. The solution is to consider the components $B$ where the series is defined and $B'$ where height goes to $-\infty$ and trace an explicit intersection path $\gamma$ between two points in these components. One can then try to infer the intersection numbers $\#(\gamma, \gamma^j)$ between $\gamma$ and every ascent path $\gamma^j$ from every critical point $\boldsymbol{p}_j$. If successful, this identifies $\mathbf{W}$ as the set of $\boldsymbol{p}_j$ such that $h(\boldsymbol{p}_j)$ is maximized among $\boldsymbol{p}_j$ such that $\#(\gamma, \gamma^j) = \pm 1$.

**Example 9.37.** The generating function $1/Q(x, y)$, where

$$Q(x,y) = 3 + x + x^{-1} + y + y^{-1} + \frac{1}{2}(x + x^{-1})(y + y^{-1}) + \frac{1}{5}(x - x^{-1} + y - y^{-1}),$$

appears in the analysis of certain matrix inversions arising from Green's function computations [Wan22]. Figure 9.6 shows a plot of the amoeba of $Q$. Its Newton polygon is the convex hull of the $3 \times 3$ grid of lattice points with $|x| \leq 1$ and $|y| \leq 1$.

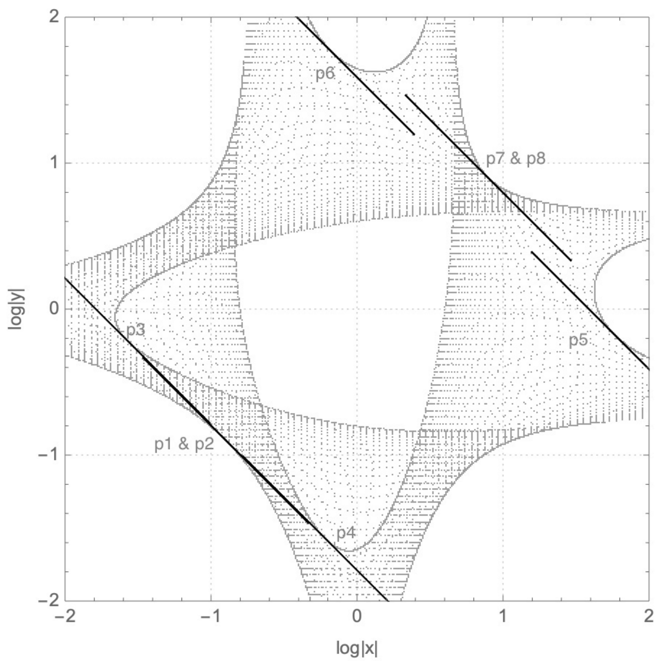


Figure 9.6 The amoeba of $Q$ (reproduced with permission of Hong-Yi Wang).

The complement of the amoeba of $Q$ has seven components, illustrated in

https://doi.org/10.1017/9781108874144.014 Published online by Cambridge University Press

Figure 9.6. Six of the components are unbounded and correspond to vertices on the perimeter of the Newton polygon, and the seventh component is a bounded component corresponding to the origin, which is an interior lattice point of the Newton polygon.

**Exercise 9.9.** Laurent polynomials whose Newton polygons are as in Example 9.37 can have as many as nine components in the amoeba complement. However the specific Laurent polynomial $Q(x, y)$ under consideration only admits seven.

(a) Let $Q_{x+}(x, y)$ denote the sum of the three monomials in $Q$ that have $x$-degree 1. How many distinct values do the magnitudes of the roots of $Q_{x+}(y)$ take?
(b) Let $Q_{x-}(x, y)$ denote the sum of the three monomials of $Q$ that have $x$-degree $-1$. How many distinct values do the magnitudes of the roots of $Q_{x-}(y)$ take?
(c) Explain why there is only one amoeba 'tentacle' in the negative $x$ direction whereas there are two in the positive $x$ direction.

Continuing our current example, the component unbounded in the $(-1, -1)$ direction corresponds to a power series expansion. However, the series of combinatorial interest in this case is the one corresponding to the bounded component, which we call $B$. Specifically, asymptotics of this series in the $(1, 1)$ direction are desired. For the component $B'$ we may choose any where $h_{(1,1)}$ is unbounded from below, and for specificity we choose the component in the upper right.

A quick computation shows the variety $\mathcal{V}_Q$ to be smooth and identifies eight critical points in the direction $\hat{\boldsymbol{r}}$ parallel to $(1, 1)$. Their projections under the Relog map are shown on the amoeba in Figure 9.6 and denoted by $\boldsymbol{p}_1, \ldots, \boldsymbol{p}_8$. All but two of the points, $\boldsymbol{p}_3$ and $\boldsymbol{p}_4$, are on the boundary of the amoeba, and the four points $\boldsymbol{p}_2 = \overline{\boldsymbol{p}_1}$ and $\boldsymbol{p}_8 = \overline{\boldsymbol{p}_7}$ come in conjugate pairs.

As described immediately prior to the example, we choose an explicit intersection cycle $\gamma$ by moving the product of circles represented by the point $\boldsymbol{x} \in B$ to one represented by a point in $B'$. The size of a fiber $\texttt{amoeba}^{-1}(\boldsymbol{x})$ for $\boldsymbol{x} \in B$ only changes when crossing a point of the amoeba contour drawn in Figure 9.6, so by sampling points and performing algebraic computations it is possible to determine that the interior of the amoeba has four regions on which the log-modulus map from $\mathcal{V}$ to $\texttt{amoeba}(Q)$ is two-to-one, while the map is four-to-one on the remainder of the amoeba (the four-to-one regions are more heavily shaded in Figure 9.6).

To construct the intersection cycle $\gamma$, we first choose $\boldsymbol{x}$ to be the origin and move it in the $(1,0)$ direction halfway to $\boldsymbol{p}_5$, then up and around the boundary of the component containing $\boldsymbol{p}_5$ moving rightward to the edge of the picture and then upward into $B'$. Until the very end, this traces a single path in each of the two preimages of the log-modulus map. Therefore $\gamma$ will be a single arc, centered on the preimage of the point $\boldsymbol{x}'$ where the amoeba was first entered (this boundary point having a single preimage) and extending downward until another piece of arc appears when passing through where the preimage size is four. This second arc can be made to occur below every critical point, therefore as a cycle relative to $-\infty$ the cycle $\gamma$ is a simple arc in the preimage size 2 region with $\boldsymbol{p}_5$ on its boundary.

We conclude immediately that $\boldsymbol{p}_1, \boldsymbol{p}_2, \boldsymbol{p}_3, \boldsymbol{p}_4, \boldsymbol{p}_5$, and $\boldsymbol{p}_6$ do not contribute. The first four are in fact higher than the origin, so the upward trajectories cannot possibly intersect the intersection cycle. For $\boldsymbol{p}_5$, it suffices to check that the two upward trajectories can be drawn to be disjoint from our choice of $\gamma$. Indeed, the two ascent arcs, projected to the amoeba, move initially in the $(-1,-1)$ direction, and can do so until they are higher than the highest point on the intersection cycle. Where they go after that is unclear, because upon entering the preimage size 4 region it is no longer clear which is the increasing time direction, so the image of the arcs may no longer be able to move in the $(-1,-1)$ direction. However, they are already high enough that they cannot intersect $\gamma$. By symmetry, an identical argument (choosing a different $\gamma$) shows that $\boldsymbol{p}_6$ cannot contribute.

By symmetry, $\boldsymbol{p}_7$ contributes if and only if $\boldsymbol{p}_8$ contributes. By process of elimination, because we know the asymptotics are non-zero, these both contribute. To argue this geometrically, one needs to understand where the two ascent arcs from $\boldsymbol{p}_7$ go. The description in terms of the four preimages is a little complicated, but one finds in the end that the projections of the two ascent arcs to the amoeba pass around the hole (the region $B$) in opposite ways, one to the north and one to the south. This forces the intersection number with $\gamma$ to be $\pm 1$; see [Wan22] for details.

We conclude that the intersection cycle $\gamma$ is homologous to the sum of a homology generator going downward from $\boldsymbol{p}_7$ and a homology generator going downward from $\boldsymbol{p}_8$, with properly chosen signs. The coordinates of the critical points are algebraic numbers satisfying

$$55\,x^8 + 664\,x^7 + 2840\,x^6 + 5780\,x^5 + 5610\,x^4 + 2520\,x^3 + 440\,x^2 - 44\,x - 45 = 0\,.$$

The points $p_7$ and $p_8$ are on the diagonal, conjugate to each other, with coordinates $-2.19\ldots \pm i1.10\ldots$. The two contributions have opposite phases, ultimately giving that

$$a_{n,n} \sim Cn^{-1/2}\alpha^{-n}\cos(n\theta),$$

where $\alpha = 6.03\ldots$ is the absolute value of the product of the coordinates in $\boldsymbol{p}_7$ (or equivalently the coordinates of $\boldsymbol{p}_8$) and $C$ and $\theta$ are non-zero constants. ◁

**Exercise 9.10.** Find the constants $C$ and $\theta$ for this example.

### 9.3.3 Smooth Bivariate Generating Functions with Degeneracies

Using the results of Chapter 4 we can give asymptotics for bivariate smooth point asymptotics in directions where the phase function $\phi$ vanishes to arbitrary order. For simplicity, we consider a power series expansion and assume that the dominant singularities are finitely minimal points where the numerator $P$ is nonvanishing. It is also possible to derive (more complicated) results when these conditions fail: for instance, they fail in Example 9.32 above.

Let $(x_*, y_*)$ be a smooth minimal critical point in the direction $\hat{\boldsymbol{r}}$ and assume that $Q_y(x_*, y_*) \neq 0$ so that we can parameterize $y = g(x)$ on $\mathcal{V}$ near $(x_*, y_*)$. Theorem 9.17 and (9.16) define functions $A$ and $\phi$ such that

$$x_*^r y_*^s (a_{rs} - \chi) = O\left(e^{-\varepsilon s}\right),$$

where

$$\chi(r,s) = x_*^{-r} y_*^{-s} \frac{1}{2\pi} \int_{-\varepsilon}^{\varepsilon} e^{-s\phi(\theta)} A(\theta)\, d\theta\,. \tag{9.19}$$

Let $c = c_\kappa$ denote the leading non-zero series coefficient in the expansion $\phi(x) \sim c_\kappa x^\kappa$ as $x \to 0$ and define the quantity

$$\Phi_{x_*,y_*}(\boldsymbol{r}) = -\frac{\Gamma(1/\kappa)}{2\kappa\pi}(1-\zeta)\frac{P(x_*,y_*)}{y_* Q_y(x_*,y_*)} c^{-1/\kappa} s^{-1/k} x_*^{-r} y_*^{-s}, \tag{9.20}$$

where, as in Theorem 4.1(*iii*), $\zeta = -1$ if $\kappa$ is even and $\zeta = \exp(\sigma i\pi/\kappa)$ if $\kappa$ is odd.

**Theorem 9.38.** *If $(x_*, y_*)$ is a strictly minimal critical point in the direction $\hat{\boldsymbol{r}}$ and satisfies the conditions above then as $(r,s) \to \infty$ with the distance from $(r,s)$ to the ray $\{t\hat{\boldsymbol{r}} : t \geq 0\}$ remaining bounded, there is an asymptotic series of the form*

$$a_{rs} \approx x_*^{-r} y_*^{-s} \sum_{j=0}^{\infty} \nu_j s^{(-1-j)/k}$$

*with leading term $\Phi_{x_*,y_*}(\boldsymbol{r})$. If $(x_*, y_*)$ is a finitely minimal point and all critical points with the same coordinate-wise modulus satisfy the same conditions as*

https://doi.org/10.1017/9781108874144.014 Published online by Cambridge University Press

*$(x_*, y_*)$ then an asymptotic series for $a_{rs}$ is obtained by adding the contributions of each of the critical points.*

*Proof* The asymptotic development follows from (9.19) and Theorem 4.1. It remains to check that the leading term is given by (9.20). Starting from (9.19) use Theorem 4.1 with $\ell = 0$ to get, in the notation of Theorem 4.1, the leading term

$$\begin{aligned}\chi &\sim \frac{x_*^{-r} y_*^{-s}}{2\pi} \int_{-\varepsilon}^{\varepsilon} A(x) e^{-s\phi(x)}\, dx \\ &= \frac{x_*^{-r} y_*^{-s}}{2\pi} I(s) \\ &= \frac{x_*^{-r} y_*^{-s}}{2\pi} (1-\zeta) C(\kappa, 0) A(0) (cs)^{-1/\kappa}.\end{aligned}$$

Parametrizing by $y$ means choosing coordinate $k = 2$ giving sign $(-1)^{k-1} = -1$ in $A(0) = -\dfrac{P(x_*, y_*)}{y_* Q_y(x_*, y_*)}$, and the fact that $C(\kappa, 0) = \dfrac{\Gamma(1/\kappa)}{\kappa}$ gives (9.20). □

**Example 9.39** (Cube root asymptotics)**.** Let $F(x, y) = 1/(3 - 3x - y + x^2)$ so that the set $\mathcal{V}$ is parametrized by $y = g(x) = x^2 - 3x + 3$. If $\hat{\boldsymbol{r}} = (a, 1 - a)$ then asymptotic behavior depends on whether $a$ is less than, equal to, or greater than $1/2$. When $a < 1/2$ there are two real critical points on the curve $y = g(x)$ – as $a$ increases from 0 to $1/2$ one approaches $(1, 1)$ from the left, and the other approaches $(1, 1)$ from the right (see Figure 9.7). Only the critical point on the right of $(1, 1)$ is minimal, and it determines asymptotics. When $a = 1/2$, the two critical points meet and $h$ becomes quadratically degenerate. Once $a > 1/2$, the critical points have complex conjugate coordinates and are both minimal.

Because $(1, 1)$ is a minimal point, the main diagonal has exponential rate zero, while all other directions have exponential decay at a rate that is uniform over compact subsets of directions not containing the diagonal. Implicit differentiation implies

$$g''(x) = -3\frac{x(x^2 - 4x + 3)}{(x^2 - 3x + 3)^2},$$

which vanishes when $x = 1$ as the critical point $(1, 1)$ in the main diagonal direction is degenerate. Computing further, we find that $g(x) - g(1)$ vanishes to order $\kappa = 3$ here, with $c = c_3 = g'''(1)/3! = i$. Checking the signs gives $\zeta = -e^{i\pi/3}$ and therefore

$$i^{-1/3}(1 - \zeta) = e^{i\pi/6} + e^{-i\pi/6} = 2\cos(\pi/6) = \sqrt{3}.$$

https://doi.org/10.1017/9781108874144.014 Published online by Cambridge University Press

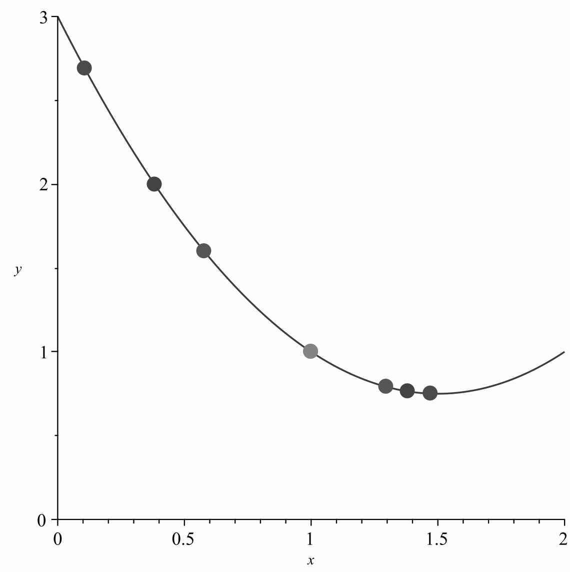


Figure 9.7 The two critical points for $Q(x, y) = 3 - 3x + x^2 - y$ in directions $(a, 1 - a)$ with $a < 1/2$, which approach the same degenerate 'double point' $(1, 1)$ when $a \to 1/2$. Only the critical points with $x > 1$ are minimal for such directions.

Evaluating $A(0) = -P(1, 1)/yQ_y(1, 1) = -1/(-1) = 1$, Theorem 9.38 gives

$$a_{r,r} \sim \frac{1}{2\pi} C(3, 0) i^{-1/3} (1 - \zeta) r^{-1/3} = \frac{\sqrt{3}\Gamma(1/3)}{6\pi} r^{-1/3} .$$

◁

**Remark.** We have given a formula holding only very near a fixed direction $\hat{\boldsymbol{r}}$. Because the results for nondegenerate smooth points hold in neighborhoods of directions, it remains to be seen whether asymptotics can be worked out that "bridge the gap" and hold when the distance $\delta = ||\boldsymbol{r} - |\boldsymbol{r}| \cdot \hat{\boldsymbol{r}}||$ to the ray $\{\lambda \cdot \hat{\boldsymbol{r}}\}$ satisfies $|\boldsymbol{r}| \gg \delta \gg 1$. See Section 13.2 for further discussion.

## 9.4 Additional formulae for asymptotics

It is sometimes useful to have alternative or more detailed formulae for the coefficients of the asymptotic expansions derived above. We collect some such formulae in this section.

https://doi.org/10.1017/9781108874144.014 Published online by Cambridge University Press

### 9.4.1 Higher order terms

We first examine explicit expressions for the higher order asymptotic coefficients.

**Theorem 9.40.** *Under the hypotheses of Theorem 9.5, the asymptotic series $\Phi_{\boldsymbol{w}}(\boldsymbol{r})$ can be expressed as*

$$\Phi_{\boldsymbol{w}}(\boldsymbol{r}) = \frac{\boldsymbol{w}^{-\boldsymbol{r}}}{\sqrt{\det(2\pi r_d \mathcal{H})}} \sum_{k\geq 0} \sum_{j=0}^{p-1} \frac{(r_d+1)_{(p-1-j)}}{(p-1-j)!\,j!} r_d^{-k} L_k(A_j, \underline{\phi}),$$

*where*

$$L_k(A,\phi) = (-1)^k \sum_{0\leq \ell \leq 2k} \left.\frac{\mathcal{D}^{\ell+k}\left(A(\boldsymbol{x})\cdot \underline{\phi}(\boldsymbol{x})^{\ell}\right)}{2^{\ell+k}\ell!(\ell+k)!}\right|_{\boldsymbol{x}=\boldsymbol{0}}$$

*for the functions*

$$\underline{\phi}(\boldsymbol{x}) = \phi(\boldsymbol{x}) - (1/2)\boldsymbol{x}\cdot\mathcal{H}\cdot\boldsymbol{x}^T$$

$$A_j(\boldsymbol{\theta}) = R_j(\boldsymbol{w}^{\circ} e^{i\boldsymbol{\theta}})$$

$$R_j(\boldsymbol{z}) = (-g(\boldsymbol{z}^{\circ}))^{-p+j} \lim_{z_d\to g(\boldsymbol{z}^{\circ})} \partial_d^j\left((z_d - g(\boldsymbol{z}^{\circ}))^p F(\boldsymbol{z})\right),$$

*and $\mathcal{D}$ is the differential operator*

$$\mathcal{D} = -\sum_{1\leq i,j\leq d} \left(\mathcal{H}^{-1}\right)_{ij} \partial_i \partial_j.$$

*Proof* Theorem 9.17 and Lemma 9.18 above imply that $\Phi_{\boldsymbol{w}}(\boldsymbol{r})$ is obtained from an asymptotic expansion of the saddle point integral (9.16), where the residue $\Psi$ is a weighted sum of terms $R_k$ occurring in the explicit formula (9.15). Distributing the integral over the sum of residue terms, Lemma 5.16 from Chapter 5 gives an asymptotic expansion of each. The stated result follows from simplifying the sum of these expansions, taking into account a subtle interplay between the lower order terms in (9.15) and the higher order terms in Lemma 5.16. □

**Remark 9.41.** It is possible to expand the falling factorials in terms of the Stirling numbers of the second kind and collect powers of $r_d$, to give an explicit formula for the coefficients $C_k$ in (9.4) at the cost of an even more unwieldy formula.

**Exercise 9.11.** In the cases $p = 1$ and $p = 2$, explicitly compute the second term in the asymptotic expansion of $\Phi_{\boldsymbol{w}}(\boldsymbol{r})$ in descending powers of $r_d$.

### 9.4.2 A geometric formula for the leading term

Complementing the explicit expressions for asymptotics given above, it is possible to write down a coordinate-free representation for the leading term using the curvature of $\mathcal{V}$ near the contributing singularities determining asymptotics. In addition to an alternative, sometimes more compact, expression, coordinate-free representations can also help with conceptual understanding, such as in Example 9.47 below. We begin by reviewing the definition of the Gaussian curvature of a smooth hypersurface, before extending it to certain points of complex algebraic hypersurfaces.

#### Gaussian curvature of real hypersurfaces

For a smooth orientable hypersurface $\mathcal{V} \subset \mathbb{R}^{d+1}$, the ***Gauss map*** $\mathcal{G}$ sends each point $\boldsymbol{p} \in \mathcal{V}$ to a normal vector $\mathcal{G}(\boldsymbol{p})$, which we identify with an element of the $d$-dimensional unit sphere $S^d$. For a given patch $P \subset \mathcal{V}$ containing $\boldsymbol{p}$, let $\mathcal{G}[P] = \cup_{\boldsymbol{q} \in P} \mathcal{G}(\boldsymbol{q})$. The ***Gaussian curvature*** (also called *Gauss–Kronecker curvature*) of $\mathcal{V}$ at $\boldsymbol{p}$ is defined as the limit

$$\mathcal{K} = \lim_{P \to p} \frac{A(\mathcal{G}[P])}{A[P]} \tag{9.21}$$

as $P$ shrinks to the single point $p$, where $A(\mathcal{G}[P])$ is the area of $\mathcal{G}[P]$ in $S^d$ and $A[P]$ is the area of $P$ in $\mathcal{V}$. When $d$ is odd, the antipodal map on $S^d$ has determinant $-1$, whence the particular choice of unit normal will influence the sign $\mathcal{K}$, which is therefore only well defined up to sign. When $d$ is even, we take the numerator to be negative if the map $\mathcal{G}$ is orientation reversing and we have a well defined signed quantity. The curvature $\mathcal{K}$ is equal to the Jacobian determinant of the Gauss map at the point $\boldsymbol{p}$.

For computational purposes, it is convenient to use standard formulae for the curvature of the graph of a function from $\mathbb{R}^d$ to $\mathbb{R}$. If $\eta$ is a homogeneous quadratic form, we let $||\eta||$ denote the determinant of the Hessian matrix of $\eta$ computed with respect to any orthonormal basis.

**Proposition 9.42** ([Bar+10, Corollary 2.4])**.** *Let $\mathcal{P}$ be the tangent plane to $\mathcal{V}$ at $\boldsymbol{p}$ and let $\boldsymbol{v}$ be a unit normal vector. Suppose that $\mathcal{V}$ is the graph of a smooth function $h$ over $\mathcal{P}$, meaning*

$$\mathcal{V} = \{\boldsymbol{p} + \boldsymbol{u} + h(\boldsymbol{u})\boldsymbol{v} : \boldsymbol{u} \in U \subseteq \mathcal{P}\}.$$

*If $\eta$ is the quadratic part of $h$, so that $h(\boldsymbol{u}) = \eta(\boldsymbol{u}) + O(|\boldsymbol{u}|^3)$, then the curvature of $\mathcal{V}$ at $\boldsymbol{p}$ is $\mathcal{K} = ||\eta||$.* □

**Corollary 9.43** (curvature of the zero set of a polynomial)**.** *Suppose that $\mathcal{V} = \{\boldsymbol{x} \in \mathbb{R}^d : Q(\boldsymbol{x}) = 0\}$ and that $\nabla Q(\boldsymbol{p}) \neq \boldsymbol{0}$. If $\eta$ is the quadratic part of $Q$ at $\boldsymbol{p}$*

https://doi.org/10.1017/9781108874144.014 Published online by Cambridge University Press

*and $\eta_\perp$ is the restriction of $\eta$ to the hyperplane orthogonal to $\nabla Q(\boldsymbol{p})$ then the curvature of $\mathcal{V}$ at $\boldsymbol{p}$ is given by*

$$\mathcal{K} = \frac{||\eta_\perp||}{||(\nabla Q)(\boldsymbol{p})||_2^{d-1}}, \tag{9.22}$$

*where $||(\nabla Q)(\boldsymbol{p})||_2$ denotes the Euclidean norm of the gradient of $Q$ at $\boldsymbol{p}$.*

*Proof* Replacing $Q$ by $||(\nabla Q)(\boldsymbol{p})||_2^{-1} Q$ leaves $\mathcal{V}$ unchanged and reduces to the case $||(\nabla Q)(\boldsymbol{p})||_2 = 1$, so we assume without loss of generality that $||(\nabla Q)(\boldsymbol{p})||_2 = 1$. Given an arbitrary vector $\boldsymbol{u}$ we write $\boldsymbol{u} = \boldsymbol{u}_\perp + \lambda(\boldsymbol{u})(\nabla Q)(\boldsymbol{p})$ to denote the decomposition of $\boldsymbol{u}$ into its components orthogonal to, and contained in, the span of $(\nabla Q)(\boldsymbol{p})$. The Taylor expansion of $Q$ near $\boldsymbol{p}$ is

$$Q(\boldsymbol{p} + \boldsymbol{u}) = (\nabla Q)(\boldsymbol{p}) \cdot \boldsymbol{u} + \eta_\perp(\boldsymbol{u}) + R,$$

where $R = O(|\boldsymbol{u}_\perp|^3 + |\lambda(\boldsymbol{u})||\boldsymbol{u}_\perp|)$. Near the origin, we can solve for $\lambda$ to obtain

$$\lambda(\boldsymbol{u}) = \eta_\perp(\boldsymbol{u}) + O(|\boldsymbol{u}|^3),$$

and the result follows from Proposition 9.42. □

**Gaussian curvature at minimal points of complex hypersurfaces**

Suppose now that $Q$ is a real polynomial in $d$ variables and that $\boldsymbol{p}$ is a minimal smooth point of the corresponding complex algebraic hypersurface. We are interested in the curvature at $\log \boldsymbol{p}$ of the logarithmic image $\log \mathcal{V} = \{\boldsymbol{z} \in \mathbb{C}^d : (Q \circ \exp)(\boldsymbol{z}) = 0\}$ of $\mathcal{V}$ (this image is similar to the amoeba of $Q$ except we do not take moduli). When $\boldsymbol{p}$ is a point with positive real coordinates then the curvature at $\log \boldsymbol{p}$ can be defined (up to a factor of $\pm 1$) directly using (9.22) from Corollary 9.43. In fact, we use this formula to define curvature in the general complex case as it is invariant under scalar multiplications of $Q$ and Theorem 6.44 from Chapter 6 implies that the normal $(\nabla_{\log} Q)(\boldsymbol{p})$ to $Q \circ \exp$ at a minimal point $\boldsymbol{p}$ is a scalar multiple of a real vector.

It is useful to observe that the curvature $\mathcal{K}$ is a reparametrization of the Hessian determinant in our asymptotic theorems, in the sense that they vanish together.

**Proposition 9.44.** *The quantity $\mathcal{K}$ defined by* (9.22) *vanishes if and only if the determinant of the Hessian matrix $\mathcal{H}$ in Theorem 9.5 vanishes.*

*Proof* Going back to its original definition in Lemma 8.22, the matrix $\mathcal{H}$ in Theorem 9.5 is the Hessian matrix for the function $g$ expressing $\log \mathcal{V}$ as a graph over the first $(d-1)$ coordinates. At such a point, the tangent plane to $\log \mathcal{V}$ is not perpendicular to the $d$th coordinate plane, and reparametrizing the graph to be over the tangent plane does not change whether the Hessian is singular. The Hessian matrix obtained from such a reparametrization represents the quadratic form $\eta$ in Proposition 9.42, so singularity of the Hessian matrix from Theorem 9.5 is equivalent to singularity of $\eta$ in Proposition 9.42. □

**Theorem 9.45** (Main Theorem of Smooth ACSV (Curvature Version))**.** *Let $F(\boldsymbol{z}) = P(\boldsymbol{z})/Q(\boldsymbol{z})$ be the ratio of coprime polynomials with convergent Laurent series expansion $F(\boldsymbol{z}) = \sum_{\boldsymbol{r}\in\mathbb{Z}^d} a_{\boldsymbol{r}} \boldsymbol{z}^{\boldsymbol{r}}$. Suppose there exists a compact set $\mathcal{R} \subset \mathbb{R}^d$ of directions such that $F$ has a smooth strictly minimal nondegenerate contributing point $\boldsymbol{w} = \boldsymbol{w}(\hat{\boldsymbol{r}}) \in \mathbb{C}_*^d$, where $Q_{z_d}(\boldsymbol{w}) \neq 0$ whenever $\hat{\boldsymbol{r}} \in \mathcal{R}$. Let $\mathcal{K}(\hat{\boldsymbol{r}})$ denote the Gaussian curvature of* $\log \mathcal{V}$ *at* $\log \boldsymbol{w}(\hat{\boldsymbol{r}})$. *Then*

$$a_{\boldsymbol{r}} = \left(\frac{1}{2\pi\|\boldsymbol{r}\|_2}\right)^{(d-1)/2} \boldsymbol{w}^{-\boldsymbol{r}}\, \mathcal{K}(\hat{\boldsymbol{r}})^{-1/2} \left(\frac{P(\boldsymbol{w})}{\|\nabla_{\log} Q(\boldsymbol{w})\|_2^2} + O\left(\|\boldsymbol{r}\|_2^{-1}\right)\right) \qquad (9.23)$$

*uniformly as $\|\boldsymbol{r}\|_2 \to \infty$ with $\hat{\boldsymbol{r}} \in \mathcal{R}$. The square-root of the matrix determinant is the product of the principal branch square-roots of the Jacobian of the Gauss map when the Gauss map is oriented towards $-\hat{\boldsymbol{r}}$.*

*Proof* As in the proofs above, we let $\omega = \boldsymbol{z}^{-\boldsymbol{r}-\boldsymbol{1}} F(\boldsymbol{z}) d\boldsymbol{z}$ so that

$$a_{\boldsymbol{r}} = \left(\frac{1}{2\pi i}\right)^{d-1} \int_\sigma \operatorname{Res}(\omega)$$

where $\sigma$ is an intersection class on $\mathcal{V}$. To work in log space we let $\boldsymbol{z} = \exp(\boldsymbol{\zeta})$, so $d\boldsymbol{z} = \boldsymbol{z} d\boldsymbol{\zeta}$ and

$$a_{\boldsymbol{r}} = \left(\frac{1}{2\pi i}\right)^{d-1} \int_{\tilde{\sigma}} \operatorname{Res}\left(\exp(-\boldsymbol{r}\cdot\boldsymbol{\zeta})\tilde{F}(\boldsymbol{\zeta})\, d\boldsymbol{\zeta}\right),$$

where $\tilde{F} = F \circ \exp$ and $\tilde{\sigma} = \log \sigma$. In fact, our assumptions imply that we have a simple pole, so we can pull out the factor of $\boldsymbol{z}^{-\boldsymbol{r}} = \exp(-\boldsymbol{r}\cdot\boldsymbol{\zeta})$ to obtain

$$a_{\boldsymbol{r}} = \left(\frac{1}{2\pi i}\right)^{d-1} \int_{\tilde{\sigma}} \exp(-\boldsymbol{r}\cdot\boldsymbol{\zeta}) \operatorname{Res}(\tilde{F}(\boldsymbol{\zeta})\, d\boldsymbol{\zeta}). \qquad (9.24)$$

Let $\mathcal{P}$ be the tangent space to $\log \mathcal{V}$ at the point $\boldsymbol{\zeta}_* = \log \boldsymbol{w}$. This tangent space consists of the vectors orthogonal to $\hat{\boldsymbol{r}}$, so we may locally parameterize $\log \mathcal{V}$ near $\boldsymbol{\zeta}_*$ by $\mathcal{P}$ using a representation

$$\log \mathcal{V} = \{\boldsymbol{\zeta}_* + \boldsymbol{\zeta}_\| + h(\boldsymbol{\zeta}_\|)\hat{\boldsymbol{r}} : \boldsymbol{\zeta}_\| \in \mathcal{P}\}.$$

Pick an orthonormal basis $\boldsymbol{v}^{(2)}, \ldots, \boldsymbol{v}^{(d)}$ for $\mathcal{P}$ so that a general point $\boldsymbol{\zeta} \in \mathbb{C}^d$ in a neighborhood of $\boldsymbol{\zeta}_*$ has a representation

$$\boldsymbol{\zeta} = \boldsymbol{\zeta}_* + u_1 \hat{\boldsymbol{r}} + \sum_{j=2}^{d} u_j \boldsymbol{v}^{(j)}.$$

Proposition C.8 in Appendix C implies

$$\mathrm{Res}(\tilde{F}(\boldsymbol{\zeta})\,d\boldsymbol{\zeta}) = \frac{P \circ \exp}{\partial(Q \circ \exp)/\partial u_1}\,du_2 \wedge \cdots \wedge du_{d+1}\,,$$

and the partial derivative in the direction of the gradient is the square of the magnitude of the gradient. Thus,

$$\mathrm{Res}(\tilde{F}(\boldsymbol{\zeta})\,d\boldsymbol{\zeta})(\boldsymbol{\zeta}_*) = \frac{P(\boldsymbol{w})}{\|\nabla_{\log} Q(\boldsymbol{w})\|_2^2}\,dA, \tag{9.25}$$

where $dA = d\boldsymbol{u}_{\|} = du_2 \wedge \cdots \wedge du_d$ is equal to the oriented holomorphic $(d-1)$-area form for $\log \mathcal{V}$ as it is immersed in $\mathbb{C}^d$.

Let $\lambda = |\boldsymbol{r}|$ and $\phi(\boldsymbol{\zeta}) = \hat{\boldsymbol{r}} \cdot \boldsymbol{\zeta}$ so that (9.24) becomes

$$a_{\boldsymbol{r}} = \left(\frac{1}{2\pi i}\right)^d \int_{\tilde{\sigma}} \exp(-\lambda\phi(\boldsymbol{\zeta}))\,\mathrm{Res}(\tilde{F}(\boldsymbol{\zeta})\,d\boldsymbol{\zeta})\,, \tag{9.26}$$

and let $\eta$ denote the quadratic part of $h$. By Proposition 9.42 (or Corollary 9.43) and the subsequent discussion, we see that the curvature $\mathcal{K}$ of $\log \mathcal{V}$ at the point $\boldsymbol{\zeta}_*$ with respect to the unit normal $\hat{\boldsymbol{r}}$ is given by $\|\eta\|$.

To proceed, we describe a logspace intersection cycle $\tilde{\sigma}$. One way to construct $\tilde{\sigma}$ is to pick a point $\boldsymbol{x}'$ in the component of $\mathtt{amoeba}(Q)^c$ giving the series expansion under consideration, and a point $\boldsymbol{x}''$ in a component of $\mathtt{amoeba}(Q)^c$ on which the height function $h$ is unbounded, and take the intersection cycle of $\log \mathcal{V}$ with a homotopy $\mathbf{H}$ obtained by taking a straight line from $\boldsymbol{x}'$ to $\boldsymbol{x}''$ and mapping by $\mathrm{Relog}^{-1}$. A convenient choice is to make the segment $\overline{\boldsymbol{x}'\boldsymbol{x}''}$ parallel to $\hat{\boldsymbol{r}}$. The real tangent space to $\mathbf{H}$ is then the sum of the imaginary $d$-space and the real 1-space in direction $\hat{\boldsymbol{r}}$. The tangent space to $\log \mathcal{V}$ is the sum of the real $(d-1)$-space orthogonal to $\hat{\boldsymbol{r}}$ and the imaginary $(d-1)$-space orthogonal to $\hat{\boldsymbol{r}}$. The tangent space to $\tilde{\sigma}$ is the intersection of these, which is the imaginary $(d-1)$-space orthogonal to $\hat{\boldsymbol{r}}$ – in other words, just $\mathrm{Im}\,\mathcal{P}$.

Because $\tilde{\sigma}$ is contained in the linear space $\mathrm{Im}\,\mathcal{P} + \mathbb{C} \cdot \hat{\boldsymbol{r}}$, we see that locally there is a unique analytic function $\alpha : \mathrm{Im}\,\mathcal{P} \to \mathbb{C} \cdot \hat{\boldsymbol{r}}$ such that $\boldsymbol{\zeta} + \alpha(\boldsymbol{\zeta}) \in \tilde{\sigma}$. Comparing to our parametrization above, we see that $\alpha = h$, so the quadratic part of $\alpha$ is therefore equal to $\eta$. Because our multivariate integral formulae are in terms of real parametrizations, we reparametrize $\mathrm{Im}\,\mathcal{P}$ by $\boldsymbol{\zeta} = i\boldsymbol{y}$ and $d\boldsymbol{\zeta} = i^d\,d\boldsymbol{y}$. In these coordinates, locally

$$\tilde{\sigma} = \{i\boldsymbol{y} + h(i\boldsymbol{y}) : \boldsymbol{y} \in \mathrm{Re}\,\mathcal{P}\}\,. \tag{9.27}$$

https://doi.org/10.1017/9781108874144.014 Published online by Cambridge University Press

Using $\hat{\boldsymbol{r}} \cdot \boldsymbol{y}_{\|} = 0$ and $\hat{\boldsymbol{r}} \cdot \hat{\boldsymbol{r}} = 1$, we obtain

$$\begin{aligned}\phi(i\boldsymbol{y} + h(i\boldsymbol{y})) &= \phi(\boldsymbol{\zeta}_*) + h(i\boldsymbol{y}) \\ &= \phi(\boldsymbol{\zeta}_*) + \eta(i\boldsymbol{y}) + O(|\boldsymbol{y}|^3) \\ &= \phi(\boldsymbol{\zeta}_*) - \eta(\boldsymbol{y}) + O(|\boldsymbol{y}|^3)\,.\end{aligned}$$

We know, by our assumptions, that $\phi$ is a smooth phase function whose real part has a minimum on $\tilde{\sigma}$ at $\boldsymbol{\zeta}_*$, which is $\boldsymbol{y} = 0$ in the parametrization (9.27). Applying Theorem 5.3 to (9.26) using the evaluation (9.25) then gives (9.23), where the square-root of the curvature is taken to be the reciprocal of the product of the principal square-roots of the eigenvalues of $-\eta$ in the positive $\hat{\boldsymbol{r}}$-direction, all of which have nonnegative real parts. The eigenvalues of $-\eta$ in direction $\hat{\boldsymbol{r}}$ are the same as the eigenvalues of $\eta$ in direction $-\hat{\boldsymbol{r}}$, which finishes the proof of the theorem. □

Again, minor modifications to proof extend to include the case where there are finitely many critical points on a minimizing torus.

**Corollary 9.46.** *Let $F(\boldsymbol{z}) = P(\boldsymbol{z})/Q(\boldsymbol{z})$ be the ratio of coprime polynomials with convergent Laurent series expansion $F(\boldsymbol{z}) = \sum_{\boldsymbol{r} \in \mathbb{Z}^d} a_{\boldsymbol{r}} \boldsymbol{z}^{\boldsymbol{r}}$ corresponding to the amoeba complement component $B \subset$ amoeba$(Q)^c$. Suppose there exists a compact set $\mathcal{R} \subset \mathbb{R}^d$ of directions such that for each $\hat{\boldsymbol{r}} \in \mathcal{R}$ the function $\hat{\boldsymbol{r}} \cdot \boldsymbol{x}$ is uniquely maximized at $\boldsymbol{x}_{\min} \in \overline{B}$, and that the set $\mathbf{W}$ of critical points in $T_e(\boldsymbol{x}_{\min})$ is finite, nonempty, and consists of smooth nondegenerate points where some partial derivative of $Q$ does not vanish. For each $\boldsymbol{z} \in \mathbf{W}(\hat{\boldsymbol{r}})$ write $\boldsymbol{z} = \exp(\boldsymbol{x}_{\min} + i\boldsymbol{y})$. Then*

$$a_{\boldsymbol{r}} = \left(\frac{1}{2\pi|\boldsymbol{r}|}\right)^{(d-1)/2} e^{-\boldsymbol{r}\cdot\boldsymbol{x}} \left[\sum_{\boldsymbol{z}\in\mathbf{W}(\hat{\boldsymbol{r}})} e^{-i\boldsymbol{r}\cdot\boldsymbol{y}} \frac{P(\boldsymbol{z})}{\|\nabla_{\log} Q(\boldsymbol{z})\|_2^2} \mathcal{K}(\boldsymbol{z})^{-1/2} + O(|\boldsymbol{r}|^{-1})\right]$$

*uniformly as $|\boldsymbol{r}| \to \infty$ with $\hat{\boldsymbol{r}} \in \mathcal{R}$.* □

**Example 9.47** (Quantum walk)**.** A ***quantum walk*** or ***quantum random walk*** (QRW) is a model for a particle moving in $\mathbb{Z}^d$ under a quantum evolution in which the randomness is provided by a unitary evolution operator on a hidden variable taking $k$ states. States and position are simultaneously measurable, but one must not measure either until the final time $n$ or the quantum interference is destroyed. A one-dimensional quantum walk was briefly presented in Exercise 9.8 as an example of torality. Here we illuminate the general form of asymptotics for a QRW, using Theorem 9.45 and Corollary 9.46 to qualitatively describe the probability profile of the particle at large time $n$. Further examples of QRWs are given in Chapter 12.

A QRW is defined by a $k \times k$ unitary matrix $U$ along with $k$ vectors $\boldsymbol{v}^{(1)}, \ldots, \boldsymbol{v}^{(k)}$

in $\mathbb{Z}^d$ representing possible steps of the walk. At each time step, the particle chooses a new state $j \in [k]$ and then moves by a jump of $\boldsymbol{v}^{(j)}$. The amplitude of a transition from state $i$ to $j$ is the entry $U_{i,j}$, while the amplitude of a path of $n$ steps, starting in state $i_0$ and ending in states $i_n$ is $\prod_{t=0}^{n-1} U_{i_t,i_{t+1}}$. Suppose the particle starts, at time zero, at the origin in state $i$. The amplitude of moving from $\mathbf{0}$ to a point $\boldsymbol{p}$ in $n$ time steps and ending in state $j$ is obtained by summing the amplitudes of all paths of $n$ steps having total displacement $\boldsymbol{p}$ and ending in state $j$. This description gives us everything we need to compute asymptotics of QRWs – for more on the interpretation of quantum walks, see [Amb+01; Bar+10].

The multiplicative nature of the amplitudes makes QRW a perfect candidate for the transfer matrix method, the univariate version of which was discussed in Section 2.2 and whose multivariate version will be discussed at length in Section 12.4. Let $M$ denote the $k \times k$ diagonal matrix whose $(j, j)$-entry is the monomial $\boldsymbol{z}^{\boldsymbol{v}^{(j)}}$ and let $P(\boldsymbol{p}, n)$ be the matrix whose $(i, j)$-entry is the amplitude to go from the origin in state $i$ at time zero to $\boldsymbol{p}$ in state $j$ at time $n$. Define the ***spacetime generating function***

$$F(\boldsymbol{z}) = \sum_{\substack{\boldsymbol{p} \in \mathbb{Z}^d \\ n \geq 0}} P(\boldsymbol{p}, n)(\boldsymbol{z}^\circ)^{\boldsymbol{p}} z_{d+1}^n \tag{9.28}$$

where $\boldsymbol{z}^\circ = (z_1, \ldots, z_d)$ are $d$ variables tracking walk position and $z_{d+1}$ is a variable tracking walk length. The transfer matrix method easily gives

$$F(\boldsymbol{z}) = (I - z_{d+1}MU)^{-1},$$

and the entries $F_{ij}$ are rational functions with common denominator

$$Q = \det(I - z_{d+1}MU)\,. \tag{9.29}$$

**Exercise 9.12.** Prove that $Q$ in (9.29) satisfies the strong torality hypothesis from Definition 9.20.

The component $B$ of the amoeba complement that yields a series in $z_{d+1}$ whose coefficients are Laurent polynomials in $z_1, \ldots, z_d$ is contained in the negative $z_{d+1}$ halfspace and has the origin on its boundary. Its boundary is smooth everywhere except the origin, where its dual cone $K$ has nonempty interior; see Figure 9.8. Recall the dual rate function $\beta^*$ on directions from (6.5). Whenever $\mathbf{0} \in \partial B$ we may deduce that $\beta^*(\hat{\boldsymbol{r}}) \leq 0$ with equality only possible if $\hat{\boldsymbol{r}} \in \mathtt{normal}_{\mathbf{0}}(B)$. The ***feasible velocity region of the QRW*** is the set $R \subseteq \mathbb{R}^d$ consisting of all $(r_1, \ldots, r_d)$ such that exponential growth rate $\overline{\beta}(r_1, \ldots, r_d, 1)$ from Definition 6.20 vanishes (in other words, it is the set of directions in which the chance of finding the particle roughly at that rescaled point after a

https://doi.org/10.1017/9781108874144.014 Published online by Cambridge University Press

long time decays slower than exponentially). Then $R \subseteq \Xi$, where $\Xi$ is the $r_d = 1$ slice of $\mathtt{normal}_{\mathbf{0}}(B)$ and is computed as an algebraic dual (see Example 6.50).

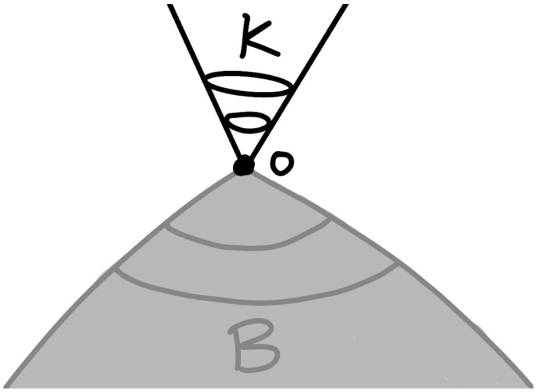


Figure 9.8 The component $B$ and its dual cone $K$ at the origin.

Smooth boundary points correspond to directions $\hat{\boldsymbol{r}} \notin K$ satisfying $|r_1| + \cdots + |r_d| < |r_{d+1}|$. For each such $\hat{\boldsymbol{r}}$ there is one or more minimal smooth critical points of $\mathcal{V}$. To compute $R$, we start by computing $\mathcal{V}_0 = \mathcal{V} \cap \mathbf{T}(\mathbf{0})$. For many QRW's one finds this to be a smooth manifold diffeomorphic to one or more $d$-tori. At any smooth point $\boldsymbol{z} \in \mathcal{V}_0$, the space $\mathbf{L}(\boldsymbol{z})$ is the line in the direction of $\nabla_{\log} Q(\boldsymbol{z})$. Thus, $\boldsymbol{r} \in R$ if and only if $\boldsymbol{r}$ is in the closure of the image when the logarithmic Gauss map $\nabla_{\log}$ is applied to $\mathcal{V}_0$, so that

$$R = \overline{\nabla_{\log}[\mathcal{V}_0]}\,.$$

This allows us to plot the feasible region by parametrizing $\mathcal{V}_0$ by an embedded grid and applying $\nabla_{\log}$ to each point of the embedded grid, an example of which is shown on the left of Figure 9.9.

The right of Figure 9.9 shows an intensity plot of the magnitude of the probability amplitude for the particle at time 200 for a QRW known as $S(1/8)$. The agreement of the shape of the empirically plotted feasible region (right) with the theoretical prediction based on the Gauss map (left) is apparent. What is also apparent is that not only do the regions agree but their fine structure of darker bands and light areas agree as well.

In particular, the image of $\mathcal{V}_0$ under $\nabla_{\log}$ will be more intense in places where the Jacobian determinant of $\nabla_{\log}$ is small because the density of the image of an embedded grid is proportional to the inverse of the Jacobian determinant. The Jacobian determinant of the logarithmic Gauss map is precisely the curvature, as discussed following (9.21). In Theorem 9.45, while

https://doi.org/10.1017/9781108874144.014 Published online by Cambridge University Press

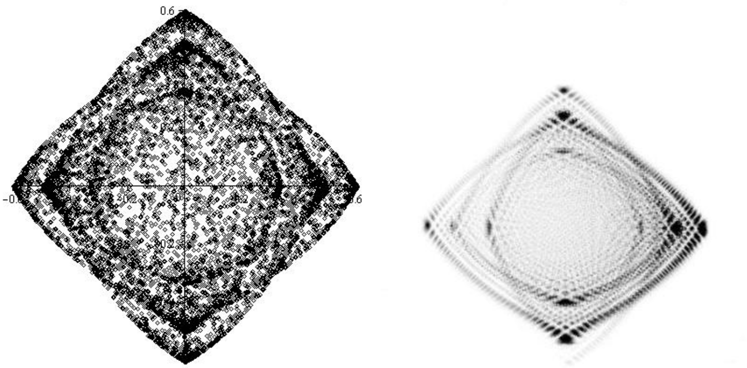


Figure 9.9 *Left:* The log-Gauss map on an embedded grid. *Right:* Probability amplitudes of a QRW.

the $P/\|\nabla_{\log} Q\|_2^2$ term varies a little, the dominant factor is the curvature term $\mathcal{K}^{-1/2}$. This explains why the density of the Gauss-mapped grid is a good surrogate for the probability amplitudes. ◁

Changing the matrix $U$ or the vectors $\boldsymbol{v}^{(j)}$ changes the walk, hence there are many quantum walks, most of which don't have the symmetries of the $S(1/8)$ walk. Figure 9.10 shows the feasibility region for a more-or-less generic quantum walk. Again, one sees an image of the logarithmic Gauss map. It is notable that, as for many quantum random walks, the feasible region is nonconvex, indicating that parts of the cone $\mathtt{normal}_{\mathbf{0}}(B)$ do not correspond to any minimal points, but are instead in the region of exponential decay (the infeasible region).

## Notes

Precursors to the derivations of the saddle point residue integrals in this chapter were the multivariate asymptotic results [BR83]. Breaking the symmetry among the coordinates, they wrote

$$F(\boldsymbol{z}) = \sum_{n=0}^{\infty} f_n(\boldsymbol{z}^\circ) z_d^n$$

for $(d-1)$-dimensional series $f_n(\boldsymbol{z}^\circ)$ and then used the fact that $f_n$ is sometimes asymptotic to an $n^{th}$ power $f_n \sim C \cdot g \cdot h^n$ to obtain Gaussian asymptotics when certain minimality conditions are satisfied near a smooth critical point. Their

https://doi.org/10.1017/9781108874144.014 Published online by Cambridge University Press

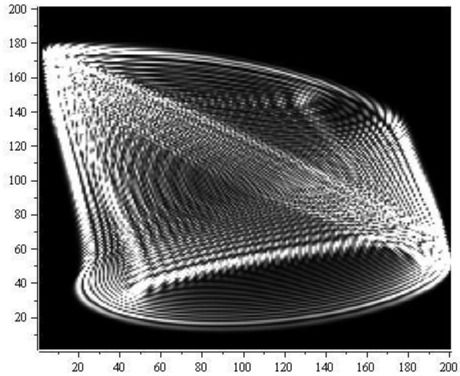


Figure 9.10 Intensity plot for a quantum walk without symmetries.

language is inherently one-dimensional, so geometric concepts such as smooth point did not arise explicitly.

The results presented in this chapter were first obtained via a direct surgery approach in [PW02], and are valid only for finitely minimal critical points. In addition, the minimality hypothesis in [PW02, Theorem 3.5] (and in many other results there) assumes an ordinary power series. The residue version of these computations appeared in print first in [Bar+10]. Extending the validity of the coordinate version beyond the case of finite intersection of $\mathcal{V}$ with $T(\boldsymbol{x}_{\min})$ was accomplished in [BP11].

Between the first and second editions of this book, a rigorous Morse theoretic foundation developed in [BMP22] streamlined some of the presentation of this chapter. The finite criticality hypothesis in this second edition replaces the strong torality hypothesis from the first edition; there, the latter is simply called *torality*. The explicit formula for higher order terms in Theorem 9.40 was first given by Raichev and Wilson [RW08]. Attempts to extend Algorithm 3 are an ongoing topic of research by an AMS Mathematics Research Community started in 2021.

The pictures in Figure 9.9 were first produced by a Penn graduate student, Wil Brady, in an attempt to produce rigorous computations verifying the limit shapes of feasible regions that were suspected from simulations. At that time, Theorem 9.45 was not known. The fact that the fine structure of the two plots agreed was a big surprise, and led to reformulated estimates such as (9.23) in terms of curvature.

Another rewriting of the leading term of the basic nondegenerate smooth point asymptotic formula is given in [Ben+12, Appendix B].

https://doi.org/10.1017/9781108874144.014 Published online by Cambridge University Press

## Additional exercises

**Exercise 9.13.** Let Res be the residue map on meromorphic forms with simple poles on a smooth variety $V$, as defined in Proposition C.6. Prove that Res is functorial, meaning it commutes with bi-holomorphic changes of coordinate.

**Exercise 9.14.** Let $f(x, y) = x^2 - 3x + 3 - y$. In Example 9.39, asymptotics in the diagonal direction reveal a quadratic degeneracy. To see what a quadratic degeneracy means topologically, begin by computing the critical points in the direction $\boldsymbol{r} = (r, 1 - r)$ as a function of $r$ on the unit interval. There should usually be two critical points. At what value $r_*$ of $r$ is there a single critical point of multiplicity 2? Check whether this is the same $r$ for which the quadratic term of $h_{\hat{\boldsymbol{r}}}$ near the critical point $\boldsymbol{z}(\hat{\boldsymbol{r}})$ vanishes.

**Exercise 9.15.** Let $F(x, y) = 1/(1 - x - y)^\ell$. Compute the asymptotics for the power series coefficients $a_{rs}^{(\ell)}$ and find the relation between these and the asymptotics of the binomial coefficients $a_{rs}^{(1)} = \binom{r+s}{r,s}$. Verify this combinatorially by finding the exact value of $a_{rs}^{(\ell)}$. *Hint:* When $\ell = 2$, the bivariate convolution of the binomial array with itself can be represented as divisions of $r + s$ ordered balls into $r$ balls of one color and $s$ of another, with a marker inserted somewhere dividing the balls into the two parts.

**Exercise 9.16.** (higher-order cube root asymptotics) In Example 9.39, dividing the error when approximating the sequence by its leading asymptotic term by the leading asymptotic term gives $0.00111\ldots$ when $r = 100$, hinting at the fact that the next nonvanishing asymptotic term is $r^{-m/3}$ for some $m$ greater than 2. Compute enough derivatives of $A$ and $\phi$ at zero to determine the next nonvanishing asymptotic term for $a_{rr}$.